Caspase-1 Mediated Pro-inflammatory Cytokine Pathway in Highly Pathogenic H5N1 Avian Influenza Infection in the Non-Human Primate Model

by

Sajen Philip Solberg

BS, Philadelphia University, 2015

Submitted to the Graduate Faculty of

the Department of Infectious Diseases and Microbiology

Graduate School of Public Health in partial fulfillment

Of the requirements for the degree of

Master of Science

University of Pittsburgh

2018

UNIVERSITY OF PITTSBURGH

GRADUATE SCHOOL OF PUBLIC HEALTH

This thesis was presented

by

Sajen Philip Solberg

It was defended on

December 11, 2018

and approved by

Committee Members:

Joshua T. Mattila, PhD
Assistant Professor
Infectious Diseases and Microbiology
Graduate School of Public Health
University of Pittsburgh

Seema S. Lakdawala, PhD
Assistant Professor
Department of Microbiology and Molecular Genetics
School of Medicine
University of Pittsburgh

Phalguni Gupta, PhD
Professor and Vice Chairman
Infectious Diseases and Microbiology
Graduate School of Public Health
University of Pittsburgh

Thesis Director:
Simon Barratt-Boyes, BVSc, PhD
Professor
Infectious Diseases and Microbiology
Graduate School of Public Health
University of Pittsburgh

Caspase-1 Mediated Pro-inflammatory Cytokine Pathway in Highly Pathogenic H5N1 Avian Influenza Infection in the Non-Human Primate Model

Sajen Philip Solberg, MS

University of Pittsburgh, 2018

Abstract

Similar to human disease, inhalation of small particle aerosols of H5N1 highly pathogenic avian influenza virus by cynomologus macaques leads to fulminant pneumonia, acute respiratory disease syndrome (ARDS), and fatality. Although aspects of the viral pathogenesis are understood, many of the finer mechanisms of H5N1 disease progression remain unclear. The severity of disease and associated mortality rate highlight the necessity to better understand this public health threat and potential bioweapon. During H5N1 infection, interferon-α and proinflammatory cytokines and chemokines markedly increase in expression within lung epithelial tissue and distal airways. This profound inflammation is characteristic of the pro-inflammatory cell death pathway known as pyroptosis. Yet, the role of pyroptosis and its initiator, caspase-1, in H5N1 influenza pathogenesis is unknown. Using immunofluorescent microscopy *in situ*, I identified active caspase-1, active IL-1β, and neutrophil extracellular traps (NETs) in association with influenza A nucleoprotein. I hypothesized that after H5N1 aerosol inoculation lung epithelial cells undergo caspase-1 dependent pyroptosis, leading to recruitment signaling of neutrophils to the site of infection and the production of NETs as secondary host immune response. NETosis, or the presentation of neutrophil extracellular traps from living or suicidal neutrophils, complicates the fulminant pneumonia present during H5N1 influenza disease progression. By trapping fluid and viral particles within the lung, it is likely that NETs prevent clearance of fluid buildup and viral particles within the highly inflamed lung tissue. I

further identified and characterized apoptosis-associated speck like proteins (ASC) containing a caspase recruitment domain (CARD) within lung epithelial cells that generate IL-1β. I found that the expression of caspase-1 correlated with NET expression and disease severity after aerosol challenge. These data suggest that caspase-1 driven inflammation of lung tissues, including pyroptotic cell death, contribute to disease severity in H5N1 influenza. What's more, in terms of public health significance; these findings help clarify cellular mechanisms associated with H5N1 disease progression furthering the understanding of H5N1 disease and could support research into the identification of novel therapeutics, such as using caspase-1 inhibitors to control inflammation and prevent severe disease progression in infected subjects.

Table of Contents

List of Tables

List of Figures

List of Abbreviations

ACD	Accidental Cell Death
ADAM	A Disintegrin and Metalloproteinase
AIF	Apoptosis Inducing Factor Mitochondria Associated Factor 1
AIM	Absent in Melanoma
ARDS	Acute Respiratory Disease Syndrome
ASC	Apoptosis-associated Speck like Protein
BAL	Bronchoalveolar Lavage
BAK	BCL2 Antagonist/Killer 1
BAX	BCL2 Associated X Protein
BCL2	B Cell Lymphoma 2
BH3	BCL2 Homology 3
BID	BH3 Interacting Death Domain Antagonist
CARD	Caspase Recruitment Domain
CYD	Cyclophilin D
C-FLIP	Caspase-8 Fas Associated via Death Domain like Apoptosis Regulation
DAMPs	Danger Associated Molecular Patterns
DCC	DCC Netrin 1 Receptor
DISC	Death-inducing Signaling Complex
ECM	Extracellular Matrix
ELANE	Elastase, Neutrophil Expressed
ESCRT	Endosomal Sorting Complex Required Transport
ERK2	Mitogen Activated Protein Kinase 2
FDG	Fludeoxyglucose
GSDMD	Gasdermin D
GSDMD-C	C Terminal of Gasdermin D
GSDMD-N	N Terminal of Gadermin D
GPX4	Reduced Glutathione Dependent Enzyme Glutathione Peroxidase 4

HIN	Hematopoetic Expression, Interferon-inducible Nature, and Nuclear Localization
HRK	Hara-Kiri Protein
IAP	Inhibitor of Apoptosis Family
IMM	Inner Mitochondrial Membrane
LPS	Lipopolysaccharide
MAP2K	Mitogen-activated Protein Kinase 2
MIF	Macrophage Migration Inhibitory Factor
MLKL	Mixed Lineage Kinase Domain like Pseudo Kinase
MPO	Myeloperoxidase
MPT	Mitochondrial Permeability Transition
NAIP	NLR Family Apoptosis Inhibitory Protein
NETs	Neutrophil Extracellular Traps
PADI4	Peptidyl Arginine Deaminase 4
PAMPs	Pathogen Associated Molecular Patterns
PARP1	Poly (ADP Ribose) Polymerase 1
PET-CT	Positron Emission Tomography, Computer Tomography
PMN	Polymorphic, Nuclear Cells
PRR	Pattern Recognition Receptors
PTCH1	Sonic Hedgehog Receptor Patched 1
PS	Phosphotidyl Serine
PTPC	Permeability Transition Pore Complex
PYD	Pyrin Domain
RAF1	RAF-1 Proto-Oncogenic, Serine/Threonine Kinase (RAF1)
RCD	Regulated Cell Death
RIPK	Receptor-interacting Serine/Threonine-protein Kinase
ROS	Reactive Oxygen Species
SMAC	Secondary Mitochondrial Activator of Caspases
tBID	Truncated form of BID
TLR	Toll like Receptors
XIAP	X-linked Inhibitor of Apoptosis

Preface

I would like to thank my mentor Dr. Simon Barratt-Boyes for his consistent guidance throughout this project. His assistance and willingness to help greatly benefitted me throughout all aspects of this project, and I feel as though I cannot thank him enough.

I would also like to extend thanks to both past and present lab members within the Barratt-Boyes lab, including but not limited to: Dr. Parichat Duangkhae, Dr. Priscilla Mayrelle Da Silva Castanha, Dr. Zachary Swan, Dr. Elizabeth Wonderlich, Dr. Colt Nash, Dana Woell, Gwenddolen Kettenburg, and Subramanian Thothathri. Their assistance throughout sleepless nights and consistent unwavering moral support, and their willingness to answer any questions help greatly.

I would like to thank the members of the Center for Biologic Imaging for their help and assitance, for answering all of my questions, and helping through any difficulties throughout countless hours on the confocal microscope and during image analysis.

Finally, I would like to extend a thank you to all the IDM master and PhD students as their friendship and moral support is and still continues to be greatly appreciated.

1.0 Introduction

1.1 H5N1 Highly Pathogenic Avian Influenza

Like seasonal influenza A, H5N1 highly pathogenic avian influenza is a member of the Orthomyxoviridae family whose virus genome are composed of 8 discrete negative sense RNA strand segments [1, 2]. These segments encode: MS1 (m1) and MS2 (m2), interferon antagonist NS1, export protein NEP, hemagglutinin protein HA, neuraminidase protein NA, polymerase protein PA, polymerase proteins PB1, PB2, and PB; and PB1-F2, which is thought to induce apoptosis [1, 2]. The virion itself contains two surface glycoproteins hemagglutinin, which binds and internalizes the virion to cells, and neuraminidase, which facilitates the release of new virions from infected cells [1, 2]. Influenza subtyping is denoted by hemagglutinin and neuraminidase antigenicity. For instance, the H5 subtype denotes the hemagglutinin of H5N1 highly pathogenic avian influenza [2].

Unlike seasonal flu H5N1 influenza is normally circulated in wild or domestic populations of land fowl or waterfowl. Avian influenza virus preferentially binds to galactose linked to sialic acid via α-2,3 linkages in waterfowl or domestic birds. Human influenza strains and other mammal influenza strains typically attach to galactose linked to sialic acid via α-2,6 linkages [1, 3-5]. In human or other mammals that can be infected with H5N1 influenza, sialic acid bound to galactose via α-2,3 linkages are commonly found in the lower respiratory tract and not the upper respiratory tract; this may account for why H5N1 influenza does not readily transmit from person

to person. Typically, avian influenza is asymptomatic in avian hosts; however influenza of the H5 or H7 subtype are found to be either high or low pathogenicity and can in high pathogenicity cases lead to fatality in domestic or wild birds [1, 2].

1.2 Human Infection

The first identified human cases of H5N1 influenza occurred in May of 1997, with the infection of a 3-year-old Chinese boy as the putative index case [6, 7]. The 3-year-old initially presented with high-grade fever, dry cough, and sore throat; however, his symptoms worsened over a period of four days, until on May 16th of 1997 he was admitted to another hospital with leukopenia, respiratory distress, and hypoxemia suggestive of acute respiratory disease syndrome (ARDS) which proved fatal [6]. In November and December of the same year, 5 more patients succumbed to the disease after coming in direct contact with infected domestic fowl [6, 7].

From 1997 onwards, the disease seemingly went dormant until its reemergence in 2003, when two more individuals contracted the disease in Hong Kong [8]. Since its reemergence in 2003, greater than 850 cases worldwide have been reported, with a case fatality ratio near 50% or greater [5, 6].

In human infection, the H5N1 virus infects human alveolar epithelial cells, causing cell death, and a loss of alveolar epithelial barrier function [1, 2, 6]. This causes a viral pneumonia seen in all human cases, leading to cyanosis, hypoxemia, and pulmonary edema, characteristic of ARDS [2, 6]. In fatal cases, this can induce respiratory failure and multiple organ failure in the host [2, 6]. The etiology of this cell death and increased inflammation in the lung is not known.

1.3 Animal Models

H5N1 influenza can infect large a number of mammalian species other than humans including cats, dogs, mice, rats, ferrets, and non-human primates [9]. H5N1 influenza virus infects primarily type 2 pneumocytes, alveolar macrophages, and non-ciliated cuboidal epithelial cells in terminal bronchioles located within the lower respiratory tract of humans and other mammals [2, 4, 7]. In addition, a previous study has documented influenza a virus infection at the soft palate at the roof of the mouth [10]. However, the presentation of disease differs between various animal models, favoring certain models for scrutiny of hallmarks of disease progression such as fulminant pneumonia presentation over others.

1.4 Pathogenesis of H5N1 Influenza in Cynomologus Macaques

Our group has shown that cynomologus macaques with H5N1 influenza via aerosol route present characteristic hallmarks of disease similar to those found in human disease [9, 11]. Following a short incubation period, of 1-2 days, infection rapidly progresses to severe pneumonia due to loss of the alveolar epithelial barrier [4, 9, 11]. This is followed by ARDS and finally death due to respiratory failure. ARDS brought on by a primary viral pneumonia is principally characterized by cyanosis, hypoxemia, pulmonary edema, and an increasing rate of respiratory failure, which in cases of highly pathogenic avian influenza leads to a multiple organ failure of the host [9, 11, 12]. In stark contrast to experiments using aerosolized virus, previous studies that utilize intra-tracheal or intra-nasal inoculation via liquid suspension produced low mortality in cynomologus macaques [13-19]. In studies that use intra-tracheal inoculation, most

animals survive initial challenge and do not present normal disease symptology. The reason for these clinical differences is that liquid suspensions of H5N1 influenza fail to reach their target cells in the alveoli, and instead are cleared by the mucociliary apparatus of the upper respiratory track. Unlike liquid suspension studies however, the previous study by our group showed symptology similar to human disease after introduction of the virus by aerosolized droplets rather than by mucosal introduction [11]. Aerosolized droplets of H5N1 influenza displayed disease pathogenesis similar to human disease and lead to high mortality rate in all cynomologus macaques. This new model presents a powerful tool to study mechanisms of disease pathogenesis.

1.5 Study of Disease Mechanism

Although some mechanisms of H5N1 influenza pathogenesis are understood, mechanisms on a cellular level surrounding H5N1 influenza disease remain unclear. Emerging evidence suggests that a major factor in disease severity emerges not directly from complications from viral infection, but from the subsequent innate host response. The innate immune response to H5N1 influenza infection consists of a dramatic increase in pro-inflammatory cytokine and chemokine levels within the host's infected tissue as well as systemically. A "cytokine storm", or disproportionate release of inflammatory cytokines and chemokines within the host as a response to infection, has been suggested as a causative factor of the ARDS that is characteristic of human disease [20, 21]. Increased plasma levels of pro-inflammatory cytokines, including IL-1β, MCP-1, IL-6, IL-8 and TNF-α in both human cases and cynomologus macaques infected by aerosol support the hypothesis of a central role played by the "cytokine storm" in disease progression, but what drives this response is unclear [11].

1.6 The Inflammasome

With the high expression of pro-inflammatory cytokines during H5N1 influenza infection, cells infected with virus generate a multiprotein complex called an inflammasome. The inflammasome forms after innate immune response recognition of a pathogen by pathogen associated molecular patterns (PAMPs), or danger associated molecular patterns (DAMPs), in cases of invading microbial pathogens or endogenous cell stress respectively [22-26]. Pattern recognition receptors (PRR), such as toll-like receptors (TLRs), NOD-like receptors, Rig-like helicases, or C-type lectin receptors, are cell receptors that identify PAMPs or DAMPs in a cell's environment [22, 23, 25, 26]. Endogenous cell stresses or invading pathogens recognized through pattern associated recognition receptors (PRR) generate inflammasome formation producing inflammation at the sites of recognition. Stimuli like invading pathogens can cause absent in melanoma (AIM)-like receptors, such as AIM2 or NLRs to form oligomers leading to cleavage of pro-caspase-1 and activation of the caspase-1 scaffold [23, 25]. Once started, the caspase-1 scaffold, including active caspase-1, cleaves of pro-inflammatory IL-1 family cytokines, such as IL-1β and IL-18, and this leads to cell death by pyroptosis, a form of pro-inflammatory regulated cell death [24, 25, 27]. The potential caspase-1 mediated inflammatory cell death in H5N1 disease pathogenesis has not yet been explored. To understand this process we need to first define the different inflammasomes and cell death pathways. There are various types of inflammasomes as discussed below.

1.6.1 NLRP3 Inflammasome

Compared to other inflammasome oligomers, cryopyrin or NLRP3 has the widest array of reactivity to stimuli, which may be attributable to downstream events from initial recognition of

danger signals that activate NLRP3 rather than individual agonists [22, 23]. Most cell types that induce an NLRP3 inflammasome require priming of NLRP3, which includes lipopolysaccharide (LPS) binding to TLR4 for example. Once primed, the receptor can respond to stimuli, and inflammasome assembly begins. Such receptive stimuli include pore-forming toxins, nucleic acids; fungal, bacterial, or viral pathogens; excess of internal ATP, crystalline substances, and hyaluronan, a scaffold protein used in a variety of cell types [22, 23, 28, 29]. Cell mechanisms that induce NLRP3 activation include potassium efflux, generation of mitochondrial reactive oxygen species, translocation of NLRP3 to the mitochondria, release of mitochondrial DNA, and the release of cathepsins to the cytosol after lysosomal destabilization. However, all these mechanisms do not apply to the variety of agonists for NLRP3; the precise mechanisms after activation remain under study [23, 26]. After activation, inflammasome assembly can occur, but not without ubiquitination of apoptosis associated speck like proteins (ASC) containing a caspase recruitment domain (CARD). Inflammasome assembly begins with the NLRP3 nucleotide oligomerization binding domain, facilitating NLRP3 Pyrin containing domains to serve as a scaffold allowing pyrin-pyrin interactions with ASC. This causes the formation of filaments of ASC allowing pro-caspase to bind via c-terminal CARD interactions, causing an autoproteolytic maturation of pro-caspase-1 to its active forms [22, 23, 30].

1.6.2 NLRC4 Inflammasome

Unlike NLRP3, NLRC4 has a narrow range of stimuli that cause its activation. NLRC4 is activated through bacterial type III secretory systems. Once activated NLRC4 complexes with NLR family apoptosis inhibitory protein (NAIP), forming the NAIP-NLRC4 inflammasome [22]. For oligomerization autoinhibition of NLRC4 must be relieved; however currently it is not understood how this occurs [22, 23]. Once oligomerized, the NAIP-NLRC4 inflammasome

interacts with ASC to form filaments of ASC, like the NLRP3 Inflammasome. It is important to note that although the NLRC4 inflammasome does contain a CARD domain, the inflammasome requires ASC to be maximally efficient [23], as without ASC autoproteolytic maturation of pro-caspase-1 cannot occur.

1.6.3 AIM2 Inflammasome

The AIM2 inflammasome directly interacts with cytosolic double stranded DNA stimuli due to the HIN (hematopoietic expression, interferon-inducible nature, and nuclear localization)-200 domain [22, 26]. The AIM2 inflammasome autoinhibits itself in its inactive state, due to interaction between the two domains within the inflammasome, but can relieve the inhibition once the sugar phosphate backbone of DNA from an invading pathogen is presented [22, 26]. Once bound, the DNA displaces pyrin domain (PYD) interactions, allowing the PYD to then recruit ASC to the oligomer. The AIM2 inflammasome is not sequence specific, but accepts nonspecific sequences of dsDNA longer than 80 base pairs [22]. Once free, the PYD interacts through PYD-PYD homotypic binding with ASC, causing the formation of ASC filaments.

1.6.4 The ASC Pyroptosome

In addition to the formation of the inflammasome oligomer, ASC also can independently act as a supramolecular assembly to induce caspase-1 dependent pro-inflammatory cell death, or pyroptosis, within cells. The ASC pyroptosome is a supramolecular assembly of 1-2 μm in diameter that can form in response to pro-inflammatory stimuli independently [26, 30-32]. Primary formation of the ASC supramolecular assembly was found to be because of potassium depletion, causing the formation of an oligomer made of ASC dimers [31]. The dimers and the

oligomer itself form due to homotypic interaction between PYD domains in ASC molecules, however once formed the supramolecular assembly has supposed enhanced intermolecular attraction, leading to the formation of the ASC pyroptosome in the cytoplasm [30, 31]. The ASC pyroptosome then cleaves endogenous pro-caspase 1 generating the active form caspase-1, leading to caspase-1 dependent pyroptosis of the cell and rupture of the cellular membrane [31, 32].

1.7 Cell Death

Cell death and the variation of cell death pathways that can occur within a host's tissue is an important distinction when considering disease pathogenesis. Broadly, cell death can fall into two major categories: accidental cell death (ACD) and regulated cell death (RCD). ACD is a catastrophic instantaneous and non-regulated demise of one or multiple cell due to exposure from severe physical, chemical, or mechanical force, usually because of harm to the organism or host [33]. RCD is, as termed, associated with regulation and organism homeostasis, focusing on the health of the organism or colony, rather than the individual cell [33]. More specifically, RCD falls into several cell death pathways including more common cell death pathways: intrinsic apoptosis, extrinsic apoptosis, pyroptosis, necroptosis, and mitochondrial permeability transition (MPT)-driven necrosis. RCD also falls into less common cell death pathways such as ferroptosis, parthanatos, entotic cell death, lysosomal-dependent cell death, autophagy-dependent cell death, mitotic catastrophe, NETotic Cell death or NETosis, and immunologic cell death [33]. It is important to note, that although some RCD are less common than others they still can occur if given the correct conditions to do so. All RCD cell death pathways are summarized (Table 1), however for this thesis, only the major cell death pathways will be extensively discussed. NETotic cell death or NETosis is extensively covered in its own

section in this introduction, as it can occur suicidally, where the neutrophil dies, or vitally, where the neutrophil returns to some normal processes.

Table 1. Regulated Cell Death Pathways

Cell death Pathway	Initiated By	Hallmarks of Pathway
Intrinsic Apoptosis	BAK and BAX, mitochondrial outer membrane permeabilization (MOMP), caspase-7 and caspase-3	BAK,BAX, Cytochrome C, APAF1, pro-caspase-9, SMAC
➢ **Anoikis**	Loss of integrin dependent attachment to the extra cellular matrix, caspase-3	Specific Type of Intrinsic Apoptosis, Associated as oncosuppresive cell death, caspase-3, MOMP
Extrinsic Apoptosis	Death receptor ligand binding, Dependence receptor ligand levels falling below threshold	Death-inducing signaling complex (DISC), Caspase-8 oligomerixzation, Type 1 and Type 2 death receptor cell death pathways, Caspase-3, Caspase-7, Caspase-9 effector caspase cascade
Pyroptosis	LPS pattern recognition from gram (-) bacteria, DAMPS and microbe-associated molecular patterns	Chromatin condensation, cellular swelling, plasma membrane permeabilization, Caspase-1, Caspase-3, Caspase-5, Caspase-4, murine Caspase-11
MPT-driven Necrosis	Severe oxidative stress, Ca^{2+} ion overload	Permeability transition pore complex (PTPC), cyclophilin D (CYPD), osmotic breakdown of the inner and outer mitochondrial membranes
Necroptosis	Death receptors (ex. FAS/TNFR1), Sequential activation RIPK3 and MLKL, MLKL oligomers	RIPK3,RIPK1, MLKL, necrosome, PS exposure, ADAM protein family members
Ferroptosis	Severe lip peroxidation, reactive oxygen species, iron deficiency	Reduced glutathione dependent enzyme gluthatione perxodiase 4 (GPX4), ferroptosis-inducing agents (ex. Erastin), ferroptosis-inhibiting agents (ex. Ferrostatins).
Parthanatos	Hyper activation of poly (ADP-ribose) polymerase 1 (PARP1), severe/prolonged akylating DNA damage, oxidative stress, hypoxia, hypoglycemia, inflammatory cues, reactive nitrogen species (ex. Nitrogen oxide)	PARP1, apoptosis inducing factor mitochondria associated factor 1 (AIF), macrophage migration inhibitory factor (MIF)
Entotic Cell Death	Detachment of epithelial cells from extra cellular matrix, loss of integrin signaling, actomyosin chain formation	Engulfing of viable cells via non-phagocytic homotypic or heterotypic cells, adhesion proteins cadherin 1 (E-cadherin, catenin alpha 1 (CTNNA), actomyosin-dependent cell-in-cell internalization, lysosomes
Lysosomal-dependent Cell Death	Permeabilization of lysosomal membrane within cytosol	Proteolytic enzymes of cathepsin family, MOMP, executioner caspases
Autophagy-Dependent Cell Death	Autophagic machinery	Autophagic machinery, growth arrest, ecdysone
Autosis	Plasma membrane sodium+/potassium+ ATPase (ex. Cardiac glycosides)	Autophagic machinery
Immunologic Cell Death	Viral infection, Chemotherapeutics, Radiation Therapy, Hypericin-based photodynamic therapy	DAMPs, activate adaptive immune response in immunosuppressive hosts
Miotic Catastrosphe*	Regulated oncosuppressive machinery, Inability to complete mitosis, extensive DNA damage, mitotic machinery problems, failure mitotic checkpoints	Multinucleation, macronucleation, micronucleation, Caspase-2 *Does not always result in RCD, sometimes cellular senescence. Forms that do lead to RCD most often lead to intrinsic apoptosis

Summary of regulated cell death pathway definitions [33].

1.7.1 Intrinsic Apoptosis

Intrinsic apoptosis occurs through a series of initiator and effector caspases, including interactions with cellular components such as BCL2 pro-apoptotic and anti-apoptotic family proteins. Initiator caspases include caspase 2, 8, and 9, and are associated with the initial outer mitochondrial membrane permeabilization [25, 34]. Effector or executioner caspases: caspase 3, 6, and 7 are known for the cellular fragmentation and characteristic nuclear and cytoplasmic condensation seen in both intrinsic and extrinsic apoptosis [25, 33].

After recognition through DAMPs, b cell lymphoma 2 (BCL2) associated pro-apoptotic and anti-apoptotic family proteins initiate intrinsic apoptosis. BCL2 associated X protein (BAX) and BCL2 antagonist/killer 1 (BAK) begin initiation by pooling on the surface of the outer mitochondrial membrane [35]. BAX is normally found cycling between the cytosol and mitochondrial membrane, while BAK is normally found within the lipid bilayer of the mitochondrial membrane [36, 37]. Once DAMPs are recognized, BCL2 homology 3 (BH3)-only activator proteins can indirectly or directly activate pooling of BAX and BAK to the surface of the mitochondria [33, 36, 37]. Pooling of BAX and BAK causes dimer-dimer oligomerization of BAX forming ring like or arc like oligomer pores, causing mitochondrial outer membrane permeabilization [33, 38-40]. Anti-apoptotic members of the BCL2 family can regulate the interaction of apoptotic BCL2 factors through direct binding, however a BH3-only sensitizer, such as hara-kiri (HRK), BCL2 interacting protein, can cause outer membrane permeabilization without BAX or BAK [33, 38].

Once the outer mitochondrial membrane has been permeabilized, pro-apoptotic factors cytochrome c and secondary mitochondrial activator of caspases (SMAC) are released from the mitochondrial intermembrane space [33, 34, 41, 42]. Cytochrome C binds to apoptotic peptidase

activating factor 1 and pro-caspase 9 to form the apoptosome, which autocatalytically matures caspase 9 through CARDs [41, 42]. Caspase 9 once matured, activates caspase 7 and caspase 3, the two of which ultimately induce cellular demise [43-45]. Caspase 7 and caspase 3 cause DNA fragmentation, phosphatidylserine exposure and apoptotic bodies characteristic of the apoptotic cell death pathway [43-45].

One of the most important regulation proteins in intrinsic apoptosis is X-linked inhibitor of apoptosis (XIAP) of the inhibitor of apoptosis family (IAP). Cytosolic SMAC is necessary to prevent inhibition of apoptosis through IAPs by direct interaction. To directly interact with IAPs SMAC must undergo a proteolytic maturation allowing for the IAP binding domain to become available to prevent XIAP [33, 46, 47]. Without this interaction XIAP can directly block the caspase cascade associated with cellular demise by physically blocking caspase 9 from forming the necessary dimers, leading to inhibition of the apoptozole and subsequent inhibition of cleavage of caspases 7 and 3 [46, 47]. XIAP is the only member of the IAP family to directly prevent the caspase cascade, while other IAPs drive upregulation of anti-apoptotic factors, trigger increased expression of pro-survival NF-ƙb, or degrade SMAC prior to its proteolytic maturation [46, 47].

1.7.2 Extrinsic Apoptosis

Unlike intrinsic apoptosis, extrinsic apoptosis is an RCD initiated by binding or loss of ligands on active receptors in association with the extracellular microenvironment. Extrinsic apoptosis is driven by plasma membrane receptors which fall either into death receptor or dependence receptor categories [33, 48, 49].

Death receptors are activated once a corresponding ligand binds to the plasma membrane receptor. Death receptors, such as Fas cell surface death receptor or TNF receptor superfamily member 10a, assemble multiprotein complexes at the intracellular tail of the receptor once a corresponding ligand is recognized [33, 48, 49]. The multiprotein complex, death-inducing signaling complex, regulates functions and activation of caspase-8 or caspase-10, which form filaments leading to their autoproteolytic maturation. This autoproteolytic maturation allows for cleavage of effector caspases, caspase-7 and caspase-3, which lead to cellular demise as in intrinsic apoptosis [33, 50, 51]. Caspase-8 fas associated via death domain like apoptosis regulation (c-flip), can modulate oligomer formation of caspase-8 preventing formation of caspase-8 filaments. Caspase-8 can prevent this by cleaving the long variant of c-flip and forming a heterodimer complex, which will favor caspase-8 oligomer formation [52-54].

There are 2 types of cell death pathways which occur from death receptor activating. These cell death pathways vary by the types of cells that they can occur in. Type 1, which occurs in thymocytes and mature lymphocytes, utilizes caspase-3 and caspase-7 to drive RCD and cannot be restrained by anti-apoptotic BCL2 proteins, loss of BAX or BAK, or loss of BH3-only activator BH3 interacting death domain agonist (BID) [33, 55]. Type 2, however, is restrained by XIAP, and requires BID cleavage by caspase-8 to continue RCD [55, 56]. Cleaved BID, or truncated form of BID (tBID), will then travel to the outer mitochondrial membrane and will act as a BH3-only activator to drive caspase-9 driven BAK and BAX dependent regulated cell death [33, 57, 58].

Dependence receptors are activated once levels of specific binding ligand fall below specific threshold for the cell. Dependence receptors, such as netrin 1 receptors DCC netrin 1 receptor (DCC) and sonic hedgehog receptor patched 1 (PTCH1), normally promote cell survival and proliferation [33, 59]. However, once their respective ligand levels drop below threshold, each dependence receptor undergoes distinct lethal signaling cascades. In the case

of PTHC1 and DCC, both dependence receptors lead to caspase-9 activation and effector caspase cascades causing cellular demise [59, 60].

1.7.3 Pyroptosis

A more recently described form of cell death is pyroptosis. Associated with extracellular and intracellular homeostasis related to innate immunity, pyroptosis is an RCD commonly distinguished by morphological features such as chromatin condensation, cellular swelling, and plasma membrane permeabilization [24, 33, 61]. Pyroptosis is commonly associated with pathological conditions like lethal septic shock and is of considerable interest in innate immunity due to its pro-inflammatory nature [61, 62]. Pyroptosis is driven by caspases such as caspase-1, caspase 3, caspase 11, caspase 4 and caspase 5 after initiation from pathogen invasion [24, 61, 63].

When gram-negative bacteria invade a cell, cytosolic LPS is recognized by pattern recognition receptors (PRRs) murine caspase-11, caspase-4, and caspase-5, which when activated lead to CARD domain interactions and caspase oligomerization [24, 27]. Murine caspase-11, caspase-4, and caspase-5 act as PRRs, and after oligomerization catalyze proteolytic cleavage of the pore forming complex gasdermin-d (GSDMD), which directly mediates pyroptosis [64-66]. GSDMD normally is inactive as its two domains: the C-terminal repressor domain (GSDMD-C) and N-terminal pore-forming domain (GSDMD-N) interact with each other preventing activation [27, 33, 64]. However once cleaved, GSDMD-N can translocate to the inner leaflet of the plasma membrane where its binds to cardiolipin [67, 68]. Once bound, GSDMD-N forms pores with an inner diameter of 10-14 nanometers, made of 16 symmetric protomers, which cause rapid plasma membrane permeabilization [33, 66].

In addition, caspase-1 is associated with pyroptosis caused by bacteria and viruses, including influenza, that are recognized by DAMPs or microbe-associated molecular patterns [69]. Caspase-1 pyroptosis is important as it can cause pyroptosis cell death of macrophages leading to the formation of pore-induce intracellular traps, trapping intracellular invasive bacteria or viruses until efferocytosis or removal by phagocytes [27, 61]. After cleavage of GSDMD by any of the active caspases, pro-inflammatory IL-1β and IL-18 are released and cleaved by the active caspase. It is worth mentioning, that other N-terminal domains from other members of the gasdermin family have been shown to cause pyroptosis, as it is not gasdermin-d alone [27, 33].

1.7.4 MPT-driven necrosis

MPT-driven necrosis is an RCD characterized by abrupt loss of impermeability of the inner mitochondrial membrane (IMM) to small solutes, a rapid dissipation of transmembrane potential, and the osmotic breakdown of both mitochondrial membranes [33, 70, 71]. MPT-driven necrosis is commonly initiated by severe oxidative stress and a cytosolic overload of calcium ions resulting in characteristic necrotic cell death presentation [33, 70]. MPT-driven necrosis follows the opening of the permeability transition pore complex, a supramolecular complex assembled at the junctions between the inner and outer mitochondrial membranes [62, 72]. The precise biochemical mechanism is still under investigation and intense debate; however, it is known that cyclophilin D (CYPD) is essential for MPT induction [33, 73]. CYPDs requirement has been established by genetic tools, however it is generally agreed that it is not a part of the permeability transition pore complex's pore-forming unit [73, 74].

1.7.5 Necroptosis

Associated with specific death receptors in response to intracellular and or extracellular microenvironment disturbance, necroptosis is a form of RCD involving receptor-interacting serine/threonine-protein kinase (RIPK) 3, RIPK 1, and mixed lineage kinase domain like pseudo kinase (MLKL) [33, 75, 76]. Necroptosis is primarily related to the meditation between adaptive response and stress responses; however, it has also been associated with developmental safeguard programs, and maintenance of adult T-cell homeostasis [77, 78]. Death receptors, such as FAS cell surface death receptor and TNF superfamily receptor 1 or PRRs like TLR4 or Z-DNA binding protein 1 (ZBP1) initiate necroptosis [33, 79]. Necroptosis depends upon the simultaneous interaction of RIPK3 and MLKL, after activation of RIPK3 with RIPK1 through interaction of a death receptor such as TNFR1 [75, 80]. Interactions between RIPK3 and RIPK1 are reliant on the physical interactions between the two RIP homotypic interaction motif (RHIM) domains and the catalytic activity of RIPK1 [81-83].

If RIPK1 is unavailable, 2 methods independent of RIPK1 but dependent on RHIM domain interactions can occur. One method involves activation of death receptors or PRRs via DAMPs or double stranded RNA recognition leading to RIPK3 activation [79]. Alternatively, ZBP1 can promote type 1 interferon synthesis and NF-ƙb activation, as it acts as a sensor for cytosolic DNA [84].

Once activated, RIPK3 catalyzes phosphorylation of MLKL leading to the formation of MLKL oligomers [80, 85]. These MLKL oligomers translocate to the plasma membrane, where they bind to specific phosphatidylinositol phosphate species, triggering the characteristic plasma membrane permeabilization [33, 85].

Oligomerization of MLKL causes a cascade of intracellular processes including an influx of calcium 2+ ions and phosphotidyl serine (PS) exposure, leading to the formation of PS bubbles on the membrane surface [85]. The breakdown of the PS bubbles is negatively regulated by endosomal sorting complex required transport (ESCRT)-III machinery [86, 87]. Once attached to the plasma membrane, MLKL activates proteases of the a disintegrin and metalloproteinase (ADAM) family initiating shedding of plasma membrane proteins and the formation of permeant magnesium 2+ channels [88, 89].

In addition, downstream activity of TNFR1 ligation promotes the formation of RIPK1-containing RIPK3 containing amyloid-like complex, known as the necrosome [81, 90]. It is important to note, that not all the core components of MLKL necroptosis are shared across animal species. Specifically, RIPK3 (but not MLKL) and MLKL (but not RIPK3) necroptosis have occur, and some species are missing one or both proteins [91, 92]. As a result, MLKL necroptosis signaling pathways are still not fully understood and require more investigation [33].

1.7.6 NETosis and NETotic Cell death

NETotic cell death is a form of RCD directly affecting polymorphonuclear neutrophils upon stimulation of specific PRRs, such as TLR4, TLR7, and TLR8 [33, 71, 93-96]. NETotic cell death is characterized by neutrophil extrusion of histone containing meshwork of chromatin fibers and granular or cytoplasmic proteins, otherwise known as neutrophil extracellular traps (NETs) [71, 93-96]. These NETs are secondary immune system responses to infection and act as a stable net of chromatin fibers in the extracellular matrix (ECM) to trap and degrade invading bacteria, viruses or fungi [71, 93-97].

NETotic cell death is initiated by PRRs on the membrane surface on the neutrophil. Once initiated, NADPH oxidases and a signaling pathways including Raf-1 proto-oncogenic, serine/threonine kinase (RAF1), mitogen-activated protein kinase 2 (MAP2K), and mitogen activated protein kinase 1 (ERK2) are induced leading the generation of intracellular reactive oxygen species (ROS) [33, 93-95]. This intracellular ROS triggers the release of elastase, neutrophil expressed (ELANE) and myeloperoxidase (MPO) from neutrophil granules in the cytosol [33, 93-95]. MPO will translocate to the nuclease where with ROS promote MPO-dependent proteolytic activity of ELANE, which aggregates of ELANE into the cells cytosol [33, 71, 93-95]. Cytosolic ELANE pools thereby catalyze proteolysis of F-actin, impairing the cells cytoskeleton, while nuclear ELANE pools in conjunction with MPO promote the degradation of histones [33, 71, 93, 98]. Additionally, nuclear ELANE pools and MPO cause chromatin decondensation, allowing for chromatin fibers to be released from the cells once the plasma membrane ruptures [33, 93, 98]. Finally, peptidyl arginine deaminase 4 (PADI4) participates in chromatin dispersion into the ECM after RCD. Some studies have suggested that NETotic cell death is partly dependent on the necroptic apparatus and inhibitors of RIPK1 and MLKL have been shown to inhibit NET formation [33, 93, 98].

Unlike NETotic cell death, NETosis, sometime referred to as “vital NETosis”, does not depend on the permeabilization of the plasma membrane and instead uses vesicular trafficking to export chromatin fibers to the ECM [94, 96]. Although not fully understood, polymorphic nuclear cells (PMNs) have been shown to rapidly release NETs and maintain cellular function, even once the cell is anuclear [33, 94, 96]. These anuclear neutrophils then act as anuclear cytoplasts to trap invading bacteria [33, 94, 96].

After release of the NETs, bacteria and viruses can be trapped via histone or nucleic acid or deoxyribose backbone interactions with the chromatin fibers [93-95, 98]. This allows the invading microbe to either be effercytosed by a phagocyte along with the remnants of the NET,

or to die without phagocytic interaction, as NETs have been shown to be microbicidal [93, 94, 97, 98]. Following removal of foreign infectious material, NETs will persist for several days, after which they are dismantled via secreted plasma nuclease DNase 1 [98, 99]. This dismantling however does not seem to fully clear the NET proteins, which persist after DNase 1 interaction, suggesting that there is another mechanism for clearance [98, 100]. Although potentially beneficial, NETs produced via NETosis or NETotic cell death have been shown to cause thrombocypenia after activation of TLRs via histones within the chromatin fibers [33, 69, 94, 98].

1.8 Previous Studies with H5N1 Influenza

Previous studies in H5N1 influenza have described apoptosis occurring at the site of infection and show high increases in pro-inflammatory cytokine generation both at the site of infection and systemically throughout the host [11, 21, 101-103]. However, there are few data to suggest that apoptosis of alveolar epithelial cells truly contributes to inflammatory cytokine generation or H5N1 disease. Instead, it appears to be more likely that pyroptotic cell death, a pro-inflammatory cell death pathway of alveolar epithelial cells, occurs at the site of infection and drives inflammatory cytokine generation.

One reason behind the lack of clarity with data generated from previous studies is the lack of an animal model that reproduces severe disease. Previous studies have demonstrated apoptosis occurring in the lower respiratory tract made use of inoculation with liquid suspensions or liquid droplets containing H5N1 HPAI via intra-tracheal or mucosal introduction [102, 103]. Unfortunately, utilizing liquid suspensions on mucosal surfaces does not allow the virus to reach the deep lung, as mucocilliary clearance prevents the virus from reaching the targeted sialic acid linkages. As well, it is possible that the way apoptosis is defined in these studies is not definitive. Wonderlich et al. shows disease progression within cynomologus

macaques more akin to human disease as the study group aerosoloized H5N1 to recapitulate natural infection and to allow the virus to reach the lower respiratory tract more easily than it can through intra-tracheal liquid suspension [11].

In addition, some studies suggest an active role of NETosis from recruited neutrophils to the site of infection [95, 104]. As previously described, NETs from NETosis are thought to be detrimental to the host as they can trap fluid, viral particles, and bacteria allowing for greater cell infections and difficulty in clearing fluid buildup prior to fulminant pneumonia. Currently there is not enough data to support this, and NETosis within H5N1 influenza requires more research.

Finally, there have been studies to suggest that H5N1 influenza interacts directly within inflammasome generation, leading to pro-inflammatory cytokine generation in tissue at the site of infection [105-109]. However, the means of which H5N1 influenza is able to do this, and which inflammasomes are being utilized by the host, are both currently understudied and require more research.

Factors including pyroptotic cell death, pro-inflammatory cytokine generation, inflammasome interaction and NETosis require research in relevant animals models during disease progression to better understand cellular mechanisms and host response to H5N1 influenza. More research into cellular mechanisms can help to better understand disease pathogenesis and illuminate possible therapeutic treatments.

2.0 Public Health Significance

Seasonal influenza A virus is a respiratory pathogen that has a large annual effect on the human population health with nearly 50,000 people dying each year in the US directly from infection or due to secondary complications associated with influenza infection [110]. While the burden of seasonal influenza disease is high, there is a larger public health concern associated with novel influenza A strains that have no prior population immunity and are not included in yearly vaccines. Such strains, like the A/2009/H1N1, could cause population-wide or nation-wide pandemics, as seen in the 2009 H1N1 influenza virus pandemic. In addition to influenza A strains with no prior immunity, strains which share an animal carrier or intermediate host are a primary focus, as the next severe pandemic could be cause by recombinant or altered strains. Highly pathogenic avian influenzas, including the H5N1 subtype, are a primary concern for potential global health threats. H5N1 influenza is a main concern due to its severe disease progression and high case fatality rate, which is greater than 50%. Although, some of the pathology of infection is understood, finer mechanisms of disease progression remain unclear. Due to its increasing incidence rate after its reemergence in 2003, H5N1 has become a primary target for public health and vaccine research to prepare for a potential species cross-overs with pandemic potential.

3.0 Specific Aims

Mechanisms that govern immune recognition and response, as well as cellular mechanisms during disease pathogenesis, in H5N1 highly pathogenic avian influenza remain unclear. To elucidate effects of H5N1 infection of the lung in cynomologus macaques this project focuses on the ability of H5N1 influenza to generate fulminant pneumonia and to induce cell death of alveolar epithelial cells. I aim to characterize cellular mechanisms occurring within the lung, to both better understand immunologic responses to H5N1 infection and to identify possible targets for therapeutics. My overarching hypothesis is that after H5N1 aerosol inoculation lung epithelial cells undergo caspase-1 dependent pyroptosis, leading to recruitment signaling of neutrophils to the site of infection and the production of NETs as secondary host immune response.

Aim 1: Characterize and Identify Caspase-1 Inflammatory Cascade within Lung of Cynomologus Macaques Infected with H5N1 Influenza Virus

This aim seeks to characterize caspase-1 inflammatory cascade within the lung of our infected H5N1 model. To start, I aim to characterized of hallmarks of caspase-1 inflammatory cascade and caspase-1 mediated pyroptosis including: caspase-1, IL-1β, and ASC expression within H5N1 infected lung tissue samples via immunofluorescent staining. In addition, I aim to quantitatively analyze areas associated with staining patterns from hallmarks of caspase-1 mediated pro-inflammatory in naïve and infected animal groups. Secondly, I aim to identify

cellular origin of IL-1β signaling via immunofluorescence, to characterize which cell types at the sites of infection express initial IL-1β after viral infection during H5N1 HPAI disease.

Aim 2: Characterize and Identify Origins of Neutrophil Signaling and NETosis within H5N1 Infected Cynomologus Macaque Lungs

This aim seeks to characterize origins of neutrophil recruitment signaling and NETs from NETosis of neutrophils within lung tissue samples. To do so I first aim to identify of Il-18 signaling from alveolar epithelial cells via immunoflourescent staining *in situ*. A second aim is to identify NETosis in lung tissue after aerosol challenge of H5N1 influenza via staining lung tissue with immunoflourescent stains of H3 histones from citrullinated histones. This is to associate NET production via innate immune responses from neutrophils to H5N1 infection.

Aim 3: Correlate Caspase-1 and NETosis to Disease Severity

This aim seeks to correlate caspase-1 and NETs from NETosis to H5N1 influenza disease severity. To do so I aim to correlate previous study data on fludeoxyglucose imagining via positron emission tomography (FDG PET-CT) scans of infected animals with Caspase-1 and NETs expression in infected tissue [11]. In addition, I aim to correlate Caspase-1 and NETs with brochiole lavage albumin levels collected from previous study data [11]. Finally, I aim to correlate caspase-1 expression with NET expression to identify if caspase-1 mediated disease is related to NET expression from recruited neutrophils.

4.0 Methods and Materials

4.1 Tissues Used in This Study

Tissue samples obtained for use in this study were collected from a previous study completed by Wonderlich et. al, in which seven adult female cynomologus macaques were exposed to live viral strain A/Vietnam/1203/2004 aerosol within a BSL3+ laboratory. The aerosol used in the previous study were approximately 4 μm in diameter and viral titers averaged at 6.72 $\log_{10}$ PFU (Table 2) [11]. Cynomologus macaques from the previous study were exposed for 15-30 minutes duration via a head only exposure unit connected to a Aeroneb Solo nebulizer (Aerogen, Deerfield, IL) [11]. Naïve controls were obtained via an additional 3 healthy female cynomologus macaques. All animals either passed due to rapid respiratory disease, with 3 animals dying, or were euthanized, between 2 and 6 days post infection. The mean time of death due to disease progression or humane sacrifice was 3.2 days (Table 2). The tissues used in the current work were fixed in 2% paraformaldehyde for 4 hours and infused with 30% sucrose overnight prior to cryopreservation.

Table 2. Characteristics of Animal Aerosol Exposure and Naïve Controls

	Animal ID	Aerosol Viral Titer (log_{10} PFU)	Time to death (days)
H5N1 Infected	M132	7.26	3
	M133	7.17	2*
	M134	7.07	6*
	M135	6.16	3
	M136	6.46	2*
	M137	6.37	2*
	M138	6.57	4
	Mean of Infected Exposure	6.72	3.2
Naïve Controls	$M59^{+}$	-------	N/A
	$M139^{+}$	-------	N/A
	$M163^{+}$	-------	N/A

*-animal humanely Sacrificed $^{+}$ - Naïve Control Animal without aerosol exposure
Table of aerosol exposure and time to death.

4.2 Slide Preparation

Tissue slides were cut on a Cryostat microtome. The blade of the microtome was changed to ensure clean cuts prior to use. Section were cut at 6 µm, and laid against plus superfrost microscope slides with environmental heat and freezing attaching the tissue ribbons to slides. Slides were incubated overnight at -20°C prior to staining to allow rest time for newly prepared tissue sections.

4.3 *In Situ* Immunofluorescence

Immunohistochemistry was performed on sections fixed with 2% paraformaldehyde from cryopreserved tissue collected during the previous study. Sections were blocked in 5% serum prior to addition of the primary antibody for 1 hour and 30 minutes or overnight exposure depending on the primary antibody used. Between staining periods, a wash of 0.5% serum was added and removed from each section, with at least one wash incubating for at least 3 minutes. Each secondary antibody used was incubated at 4°C for one hour prior to removal. The following antibodies were used: mouse anti-pan cytokeratin (AE1/AE3; Abcam), mouse anti-human calprotectin Ab-1 (MAC397; ThermoScientific), anti-influenza A nucleoprotein (DPJY03; BEI resources), anti-IL-1β/IL-1F2 (6E10; Novus Biologics), anti-ASC (B-3, Santa Cruz Biotechnology), anti-caspase-1 p20 (C-15, Santa Cruz Biotechnology), anti-caspase-1 (D-3, Santa Cruz Biotechnology), anti-influenza A nucleoprotein polyclonal Ab (PA5-32242, ThermoScientific), anti-IL-18 (10663-1-AP, Proteintech), and anti-histone H3 (P68431, Abcam). Secondary antibodies were from Thermo Fischer Scientific and included goat anti-mouse IgG2α Alexa Fluor 488, goat anti-mouse IgG2α Alexa Fluor 647, goat anti-mouse IgG1 Alexa Fluor 546, donkey anti-goat IgG Alexa Fluor 488, donkey anti-rabbit IgG Alexa Fluor 488, and donkey anti-rabbit IgG Alexa Fluor 546. Cell nuclei were identified using membrane-permeable Hoescht dye and slides were mounted in ProLong Diamond Antifade mountant (P36965, Thermo Fischer Scientific). All staining included appropriately concentrated isotype-matched control antibody. Slides were images on Olympus Fluoview FV1000 confocal microscope from the University of Pittsburgh Center for Biologic Imaging. Images were captured at 1024 x 1024 pixels ratio at 10 pixels per microsecond at various objective focal points including: 20x, 40x, 60x, or 100x objective focus.

4.4 Image Analysis and Quantification of Staining

Quantitative analysis of dual staining patterns were used to compare statistical differences between naïve and post-infected animal groups. Tissue sections collected were not normalized for size and viral titer, as sections were collected during necropsy from the previous aerosol challenge study [11]. To normalize for size differentiation and exposure differentiation, each section was non-repetitively imaged a total of ten times per slide per stain and these quantitative results were averaged for each individual animal. These images were analyzed with Nis Elements ver. 5.11.00, and areas of active staining were quantitatively examined and recorded for each of the ten fields across the tissue. Areas of active staining were examined with binary area quantification, where each pixel of an image is given a value between 0 and 1, and the total area is then related to the total number of available pixel in the image. Binary areas of stain were averaged across the ten focal points for each tissue, and a median of staining intensity from all post-infected slides and all naïve slides was established as used for comparisons.

4.5 Statistical Analysis

All statistical analysis was performed in Prism v6.0 (GraphPad Software). A p value <0.05 was considered significant. All analysis was performed using two tailed, nonparametric tests between infected and control animals. Data collected was averaged for either post-infected or naïve control groups. The averages of $\log_{10}$ were calculated as geometric means.

5.0 Results

5.1 Aim 1

Although the actions of caspase-1 and IL-1β as well as other pro-inflammatory cytokines and chemokines have been previously elucidated during seasonal influenza, as well as through aerosolized challenge of H5N1 influenza, effects of these cytokines and their cells of origin points still require further clarification. In this vein, the first aim of this project was to identify hallmarks of the caspase-1 pro-inflammatory cascade within infected snap frozen lung tissue collected during necropsy following aerosolized challenge of H5N1 virus [11].

5.1.1 Hallmarks of the Caspase-1 Pro-Inflammatory Cytokine Cascade

5.1.1.1 Caspase-1 in Association with Influenza A Nucleoprotein

Necropsied snap frozen tissues of lung were collected at varying time points following aerosolized challenge. Tissues were sectioned and sections were stained with antibodies to caspase-1 and influenza A nucleoprotein. Sections were prepared at 6 μm and stained with a monoclonal caspase-1 immunofluorescence antibody and a polyclonal influenza A nucleoprotein antibody. Sections were examined under 40x objective focus on an Olympus Fluoview 1000 confocal microscope to identify caspase-1 and influenza A nucleoprotein co-localization. The influenza A nucleoprotein marker was chosen for its cross-reactivity with seasonal influenza A strains and our H5N1 HPAI strain, A/Vietnam/1203/2004. Co-localization

of caspase-1 and H5N1 virus was our initial step to identify pro-inflammatory cytokine generation after viral challenge.

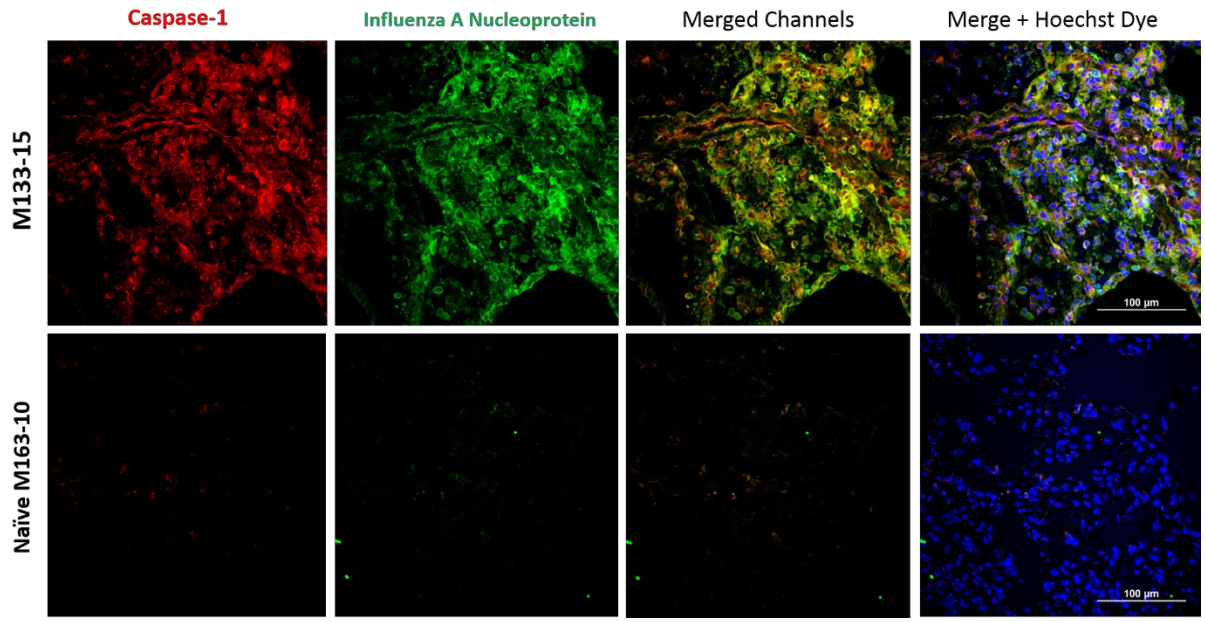

Figure 1. Caspase-1 and Influenza A Nucleoprotein Immunoflourescent Staining in situ

Infected and naïve necropsied snap frozen lung tissues stained for polyclonal active caspase-1 and monoclonal influenza A nucleoprotein. Caspase-1 was stained with Alexa fluor 546, and appears red in coloration. Influenza A nucleoprotein was stained with Alexa fluor 488, and appears green in coloration. Hoechst dye was used to identify nuclei in cells. Scale bars, 100 µm.

Following staining, each post-infection time point showed a large amount of caspase-1 and influenza A nucleoprotein, as well as high cellular condensation due to swelling from local pulmonary inflammation after aerosol challenge. Each infected macaque tissue also had high visible background of DAPI Hoeshct stain (data not shown). Hoeshct staining normally is used to identify nuclei of cells within deep lung, but this staining pattern with high visible background was attributable to large amounts of albumin and sputum generated via secondary infection and the resultant fulminant pneumonia. Naïve tissues collected from control animals during the aerosolized H5N1 mock challenge had minimal to no amount of caspase-1 expression (Figure

1). Staining co-localization suggests expression of caspase-1 mediated pro-inflammatory cytokine cascade as a result of viral infection of epithelial cells. Although minimally expressed within naïve tissue, I wished to quantitatively identify the increase in pro-inflammatory caspase-1 and compare quantitative areas of stain from both naive and infected animals.

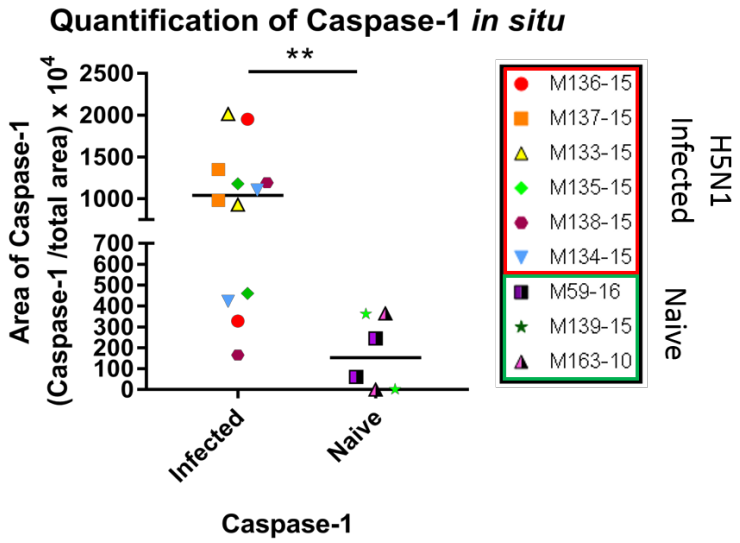

Figure 2. Quantification of Caspase-1

Quantification of caspase-1 within necropsied snap frozen tissues from post-infected and naïve animals stained with caspase-1. Data points refer to multiple dual stained sections per animal, where dual stained sections where stained either with influenza A nucleoprotein or IL-1β along with caspase-1. The *p* values were determined through Mann-Whitney U tests. *$p < 0.05$, **$p<0.01$.

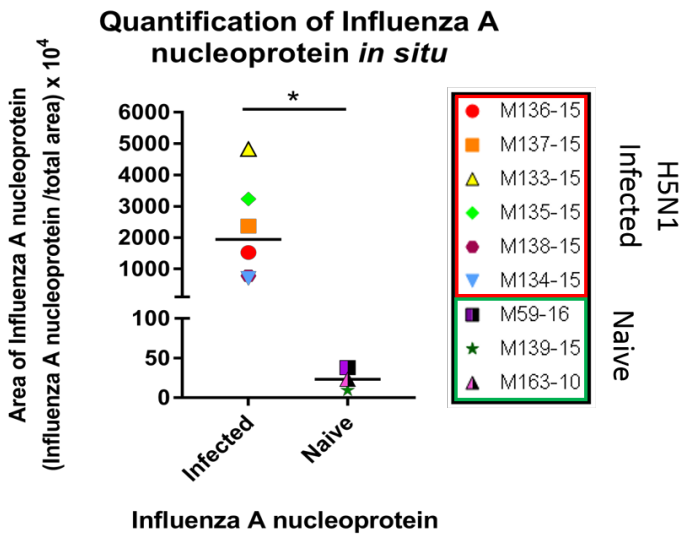

Figure 3. Quantification of Influenza A Nucleoprotein

Quantification of influenza A nucleoprotein within necropsied snap frozen tissues from post-infected and naïve animals dual stained with influenza A nucleoprotein and caspase-1. The p values were determined through Mann-Whitney U tests. *$p < 0.05$.

When comparing the infected and naïve animal groups a statistical increase in caspase-1 expression was present in infected tissue sections (Figure 2). Influenza A nucleoprotein was also determined to have a statistical increase when compared against our naïve slides (Figure 3). Furthermore, we analyzed the staining of caspase-1 alone versus caspase-1 that co-localized with influenza a nucleoprotein in deep lung tissue sections, and found that caspase-1 within infected animal tissues, was statistically found to be co-localized with influenza A nucleoprotein rather than un-associated with influenza A nucleoprotein (Figure 4). Co-localization of caspase-1 and influenza A nucleoprotein suggests caspase-1 mediated pro-inflammatory cytokine cascade expression after viral challenge (Figure 4).

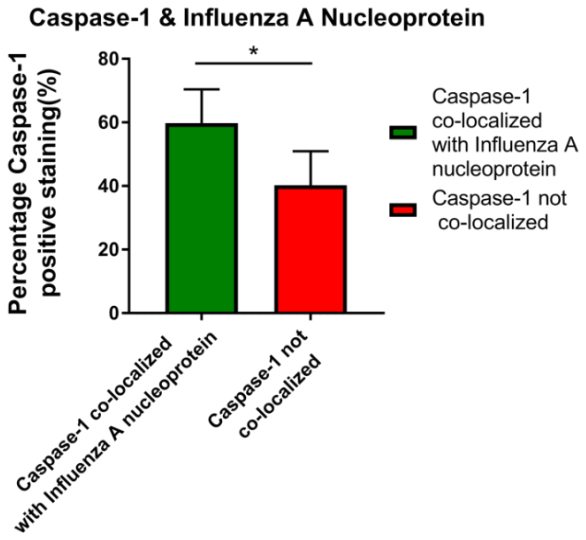

Figure 4. Quantification *of* Co-localization of Caspase-1 and Influenza A Nucleoprotein

Quantification of co-localization of caspase-1 with influenza A nucleoprotein. The *p* values were determined through Mann-Whitney U tests. *$p < 0.05$

5.1.1.2 Caspase-1 in associated with IL-1β

After identification of caspase-1 and influenza A nucleoprotein within our infected and naïve tissue, we wanted to correlate the staining of caspase-1 and IL-1β to identify both the primary and secondary hallmarks of the caspase-1 pro-inflammatory cytokine cascade leading to potential pyroptotic cell death of tissue within our deep lung sections. To do so necropsied tissues collected from the previous study were sectioned and stained with monoclonal antibodies specific for active caspase-1 and IL-1β. Co-localization of the stains was observed and quantitatively analyzed (Figures 5 and 6).

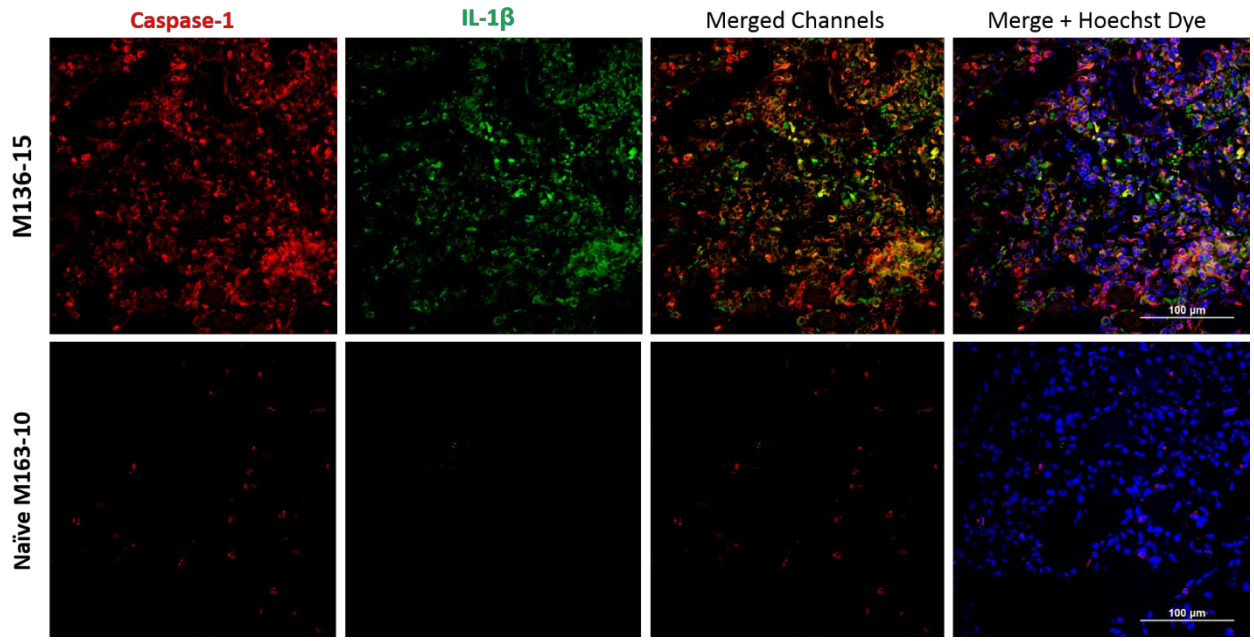

Figure 5. Caspase-1 and IL-1β Immunoflourescent Staining in situ

Infected and naïve necropsied snap frozen deep lung tissues stained for monoclonal active caspase-1 and monoclonal active IL-1β. Caspase-1 was stained with Alexa fluor 546, and appears red in coloration. IL-1β was stained with Alexa fluor 647, and appears green in coloration. Hoechst dye was used to identify nuclei in cells. Scale bars, 100 µm.

Similar to our caspase-1 staining in tissues, IL-1β staining showed a statistical increase between naïve and post-infected tissues (Figure 6). Furthermore, we analyzed the staining of IL-1β alone versus IL-1β that co-localized with caspase-1 in our deep lung tissue. We found that IL-1β within the tissues that were imaged was statistically non-co-localized with caspase-1 (Figure 7). This data further supports caspase-1 mediated pro-inflammatory cytokine cascades after vial challenge. This data suggests that there is not a one to one correlation between active caspase-1 and active IL-1β. Pro-IL-1β is normally cleaved by active caspase-1, suggesting each active caspase-1 substrate may cleave more than one pro-IL-1β.

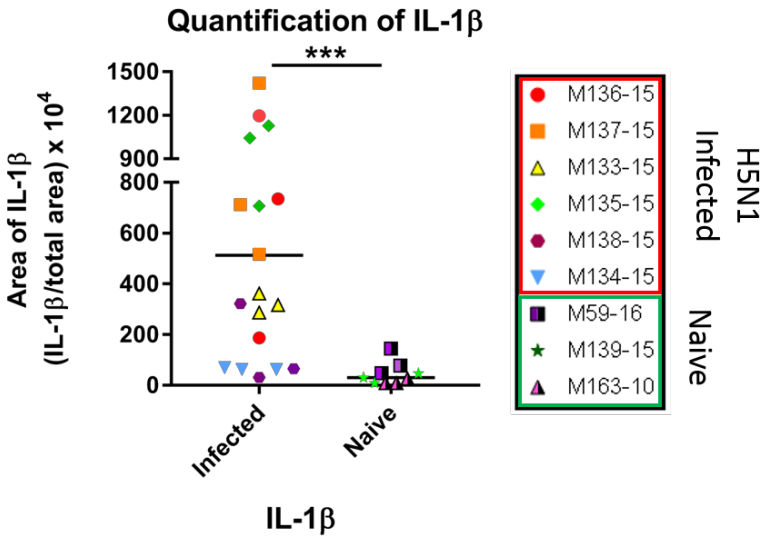

Figure 6. Quantification of IL-1β

Quantification of IL-1β within necropsied snap frozen tissues from post-infected and naïve animals stained with IL-1β. Data points refer to multiple dual stained sections per animal, where dual stained sections where stained either with caspase-1, anti-H3 histones, or anti-ASC along with IL-1β. The *p* values were determined through Mann-Whitney U tests. *$p < 0.05$, **$p<0.01$,***$p < 0.0001$.

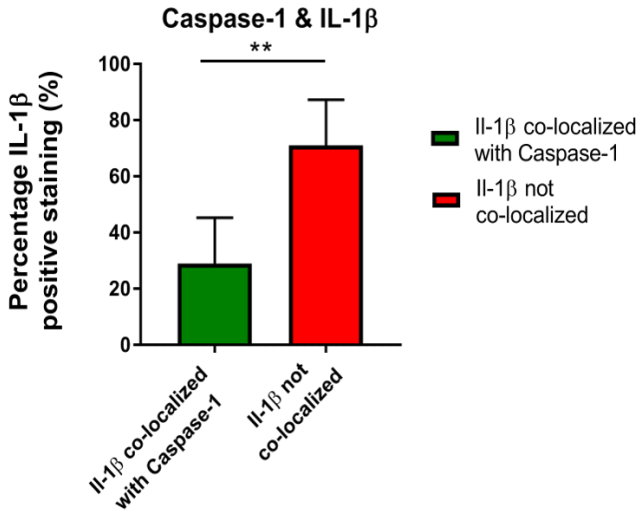

Figure 7. Quantification of Co-localization of Caspase-1 and IL-1β

Quantification of co-localization of caspase-1 with IL-1β. The *p* values were determined through Mann-Whitney U tests. *$p < 0.05$, **$p<0.01$.

5.1.2 Caspase-1 Mediated Pyroptotic Cell Death

5.1.2.1 ASC protein associated with IL-1β

After identifying both caspase-1 associated with our H5N1 influenza nucleoprotein and caspase-1 associated with IL-1β, we wanted to identify hallmarks of caspase-1 mediated pyroptotic cell death within our deep lung tissues. To do so I looked at a marker of inflammasome generation and a marker of pyroptotic cell death via cellular membrane rupture, apoptosis speck like protein containing a card domain, otherwise known as ASC. Sections from necropsied tissue were stained with monoclonal antibodies for ASC and active IL-1β to identify potential co-localization (Figure 8). Images collected from these sections were quantitatively analyzed via NIS elements as stated in the materials and methods section of this thesis to identify statistical differences between ASC protein in both naïve and post-infected tissues (Figure 9).

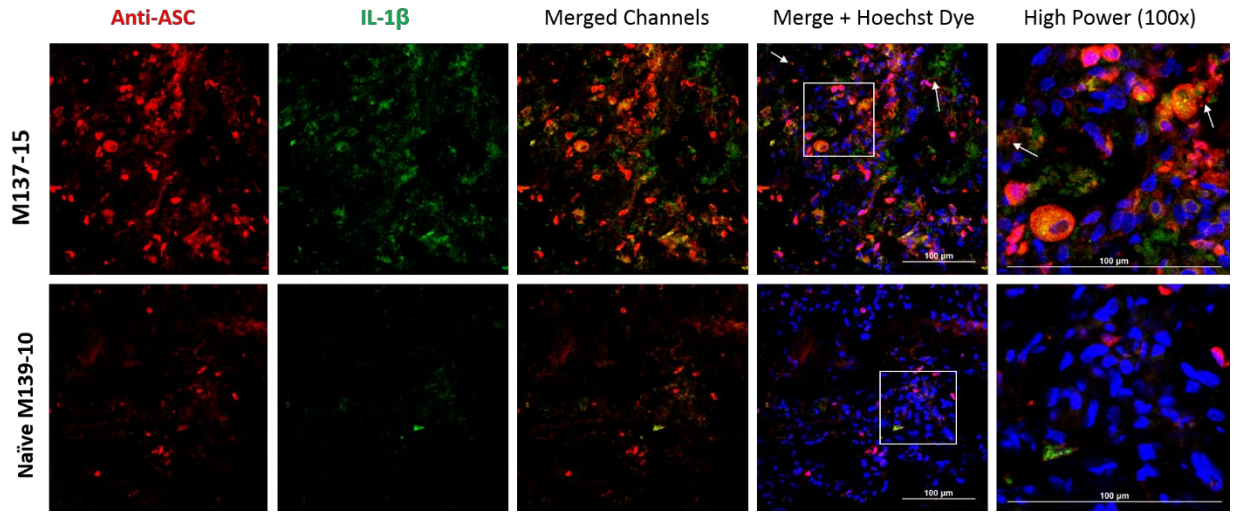

Figure 8. Anti-ASC and IL-1β Immunoflourescent Staining in situ

Infected and naïve necropsied snap frozen deep lung tissues stained for monoclonal ASC and monoclonal active IL-1β. Anti-ASC was stained with Alexa fluor 546, and appears red in coloration. IL-1β was stained with Alexa fluor 647, and appears green in coloration. Hoechst dye was used to identify nuclei in cells. Scale bars, 100 µm. Arrows indicate punctate morphology from ASC oligomerization.

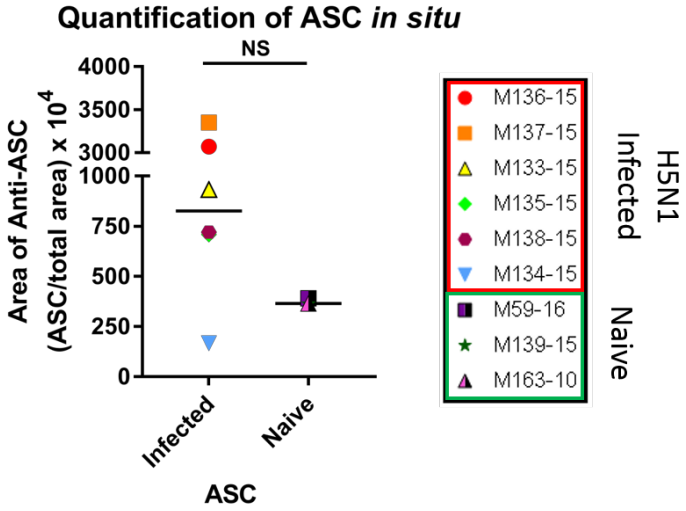

Figure 9. Quantification of Anti-ASC

Quantification of anti-ASC within necropsied snap frozen tissues from post-infected and naïve animals dual stained with anti-ASC and IL-1β. The *p* values were determined through Mann-Whitney U tests. *$p < 0.05$.

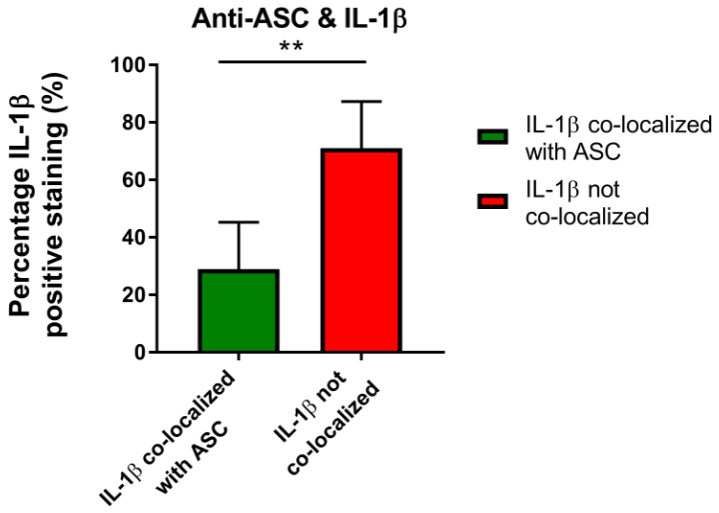

Figure 10. Quantification of Co-localization of Anti-ASC and IL-1β

Quantification of co-localization of anti-ASC with IL-1β. The *p* values were determined through Mann-Whitney U tests. *$p < 0.05$, **$p<0.01$.

ASC had no significant increase between infected and naïve animal groups (Figure 9). In immunoflourescent staining, ASC was seen as speck like puncta through some of the tissue, which may be due to the formation of ASC oligomers instead of ASC interacting with another inflammasome complex (Figure 8). When quantitatively analyzed, there was a significant difference between IL-1β which co-located and IL-1β that did not co-located with ASC, which may be due to multiple cleavages of IL-1β from individual cells (Figure 10). ASC, either in its oligomer form or in conjunction with other inflammasome complexes, is active in lung tissue with pro-inflammatory IL-1β, which suggests pyroptotic death of cells in infected tissue, such as alveolar epithelial cells.

5.1.3 Cellular Origin of IL-1β Signaling

To identify co-localized IL-1β staining with its cellular origin, and identify which cells could be potential origins of IL-1β signaling after viral challenge sections were stained for IL-1β and a cellular marker, such as cytokeratin to mark alveolar epithelial cells, calprotectin to mark neutrophils, and CD163 to mark macrophages within the lung.

5.1.3.1 IL-1β signaling from Alveolar Epithelial Cells

In dual stains with cytokeratin as a marker for alveolar epithelial cells we saw clear co-localization visible in an orange color due to the overlap of our Alexa Fluor 488 green stain and our red Alexa Fluor 546 staining (Figure 11). Importantly, a large amount of co-localization seems to occur in alveolar epithelial cells, which outline alveolar spaces, and in some of the terminal bronchioles that could account for large amount of recruited cells seen in BAL fluids obtained from the previous study. This data suggests that IL-1β cytokine signaling is generated from alveolar epithelial cells, and that these alveolar epithelial cells are generating pro-inflammatory cytokines after viral challenge.

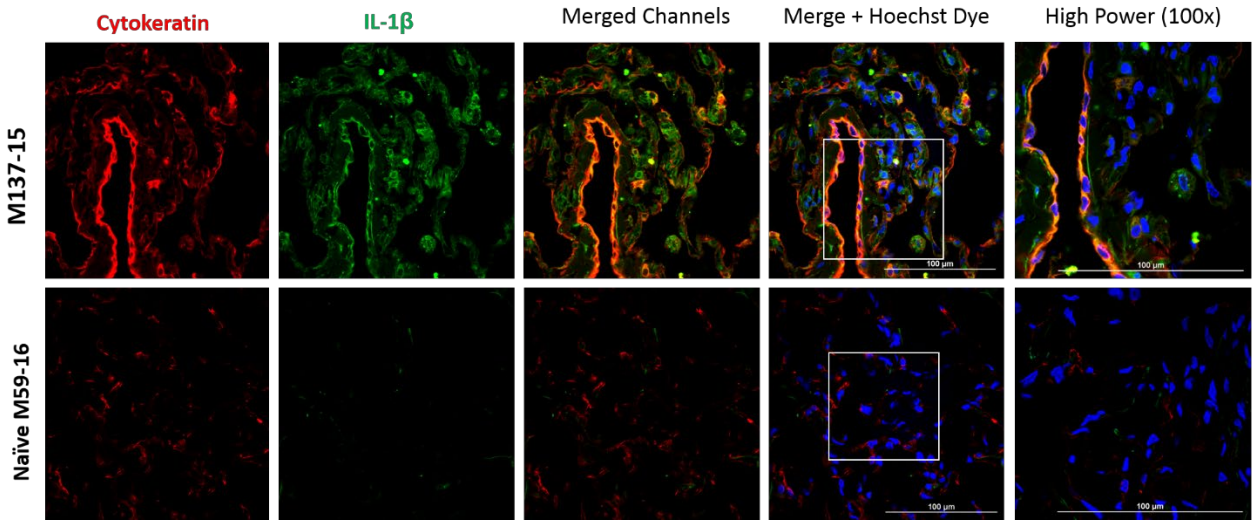

Figure 11. Cytokeratin and IL-1β Immunoflourescent Staining in situ

Infected and naïve necropsied snap frozen deep lung tissues stained for monoclonal cytokeratin, to mark alveolar epithelial cells, and monoclonal active IL-1β. Cytokeratin was stained with Alexa fluor 546, and appears red in coloration. IL-1β was stained with Alexa fluor 647, and appears green in coloration. Hoechst dye was used to identify nuclei in cells. Scale bars, 100 µm.

5.1.3.2 IL-1β signaling from Neutrophils

Similar to our cytokeratin staining, we saw clear co-localization between calprotectin, a marker for neutrophils recruited to the site of infection, and IL-1β (Figure 12). Neutrophils at the site of infection appear to generate pro-inflammatory cytokines, such as IL-1β, in areas of infected tissue.

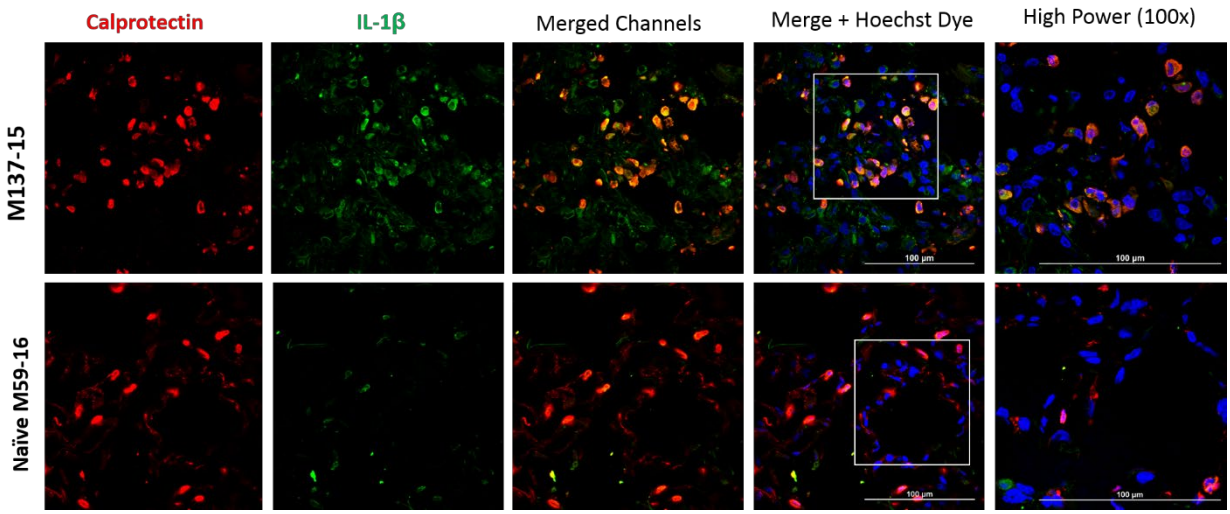

Figure 12. Calprotectin and IL-1β Immunoflourescent Staining in situ

Infected and naïve necropsied snap frozen deep lung tissues stained for monoclonal calprotectin, to mark alveolar recruited or alveolar neutrophils, and monoclonal active IL-1β. Calprotectin was stained secondarily with Alexa fluor 546, and appears red in coloration. IL-1β was stained secondarily with Alexa fluor 647, and appears green in coloration. Hoechst dye was used to identify nuclei in cells. Scale bars, 100 µm.

5.1.3.3 IL-1β signaling from Macrophages

CD163, a macrophage marker for alveolar macrophages and macrophages recruited to the site of infection, was stained in tissue alongside IL-1β. Unlike our previous cell markers, there is no apparent co-localization of CD163 and IL-1β, however there is a large recruitment of macrophages to the site of infection compared to our naïve tissue sections (Figure 13). Pro-inflammatory cytokine generation does not appear to orginate from macrophages at the site of infection, even with large populations of macrophage within infected deep lung tissue.

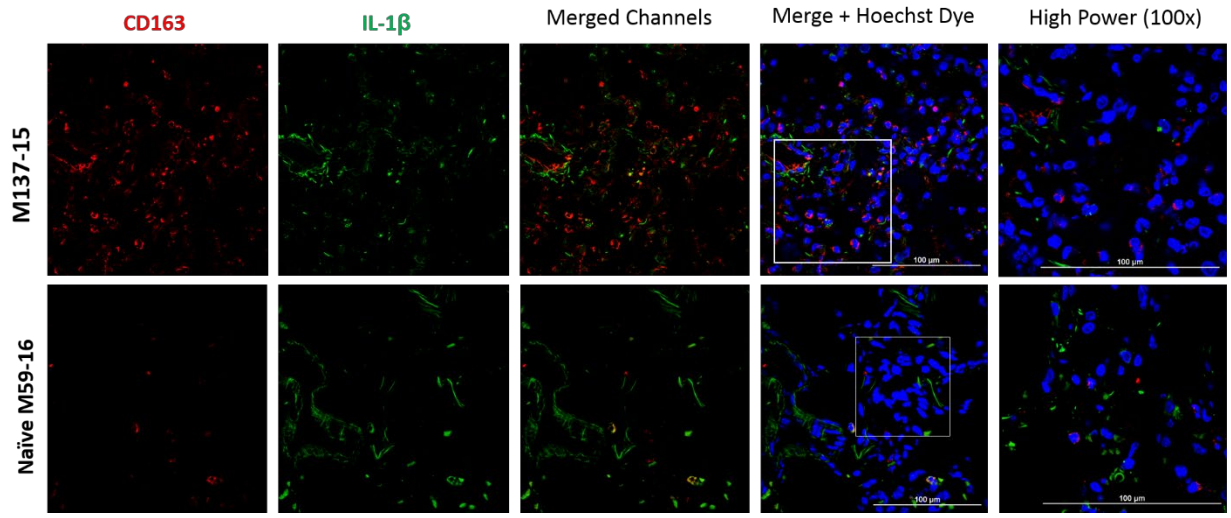

Figure 13. CD163 and IL-1β Immunoflourescent Staining in situ

Infected and naïve necropsied snap frozen deep lung tissues stained for monoclonal CD163, to mark alveolar macrophages, and monoclonal active IL-1β. CD163 was stained secondarily with Alexa fluor 546, and appears red in coloration. IL-1β was stained secondarily with Alexa fluor 647, and appears green in coloration. Hoechst dye was used to identify nuclei in cells. Scale bars, 100 µm.

5.1.4 Aim 1 Conclusions

At the conclusion of aim 1, I found that high expression of caspase-1 co-localized with influenza A nucleoprotein suggest a correlation between caspase-1 mediated pro-inflammatory cytokine generation and H5N1 influenza disease. This conclusion was further support by high expressions of IL-1β and ASC *in situ*, which suggest caspase-1 mediated pro-inflammatory cytokine generation and caspase-1 mediated pyroptosis in infected tissues. Finally, I found that co-localizations of IL-1β and cytokeratin or calprotectin, our markers for epithelial cells and neutrophils, suggest that both alveolar epithelial cells and neutrophils express IL-1β in response to infection in lung tissue.

5.2 Aim 2

During the previous study large amounts of pro-inflammatory cytokines and chemokines were collected through bronchoalveolar lavage (BAL) fluid and tissue necropsy after aerosolized challenge of H5N1 highly pathogenic avian influenza [11]. Some effects of these cytokines and their origination points are known, however others require further clarification. The second aim of this project was twofold, first to identify IL-18 generation from alveolar epithelial cells, and secondly to identify NETosis from recruited or alveolar neutrophils at the sites of infection.

5.2.1 IL-18 Staining Within Alveolar Epithelial Cell Sections

IL-18 is hypothesized to act as the recruitment cytokine signaling for recruited neutrophils within the deep tissue of the lung. Alveolar epithelial cells were hypothesized as the origin for IL-18 expression. Identification of IL-18 in tissue sections, prepared at 6 μm thickness, was completed via staining for antibodies to IL-18 and cytokeratin, a marker for alveolar epithelial cells.

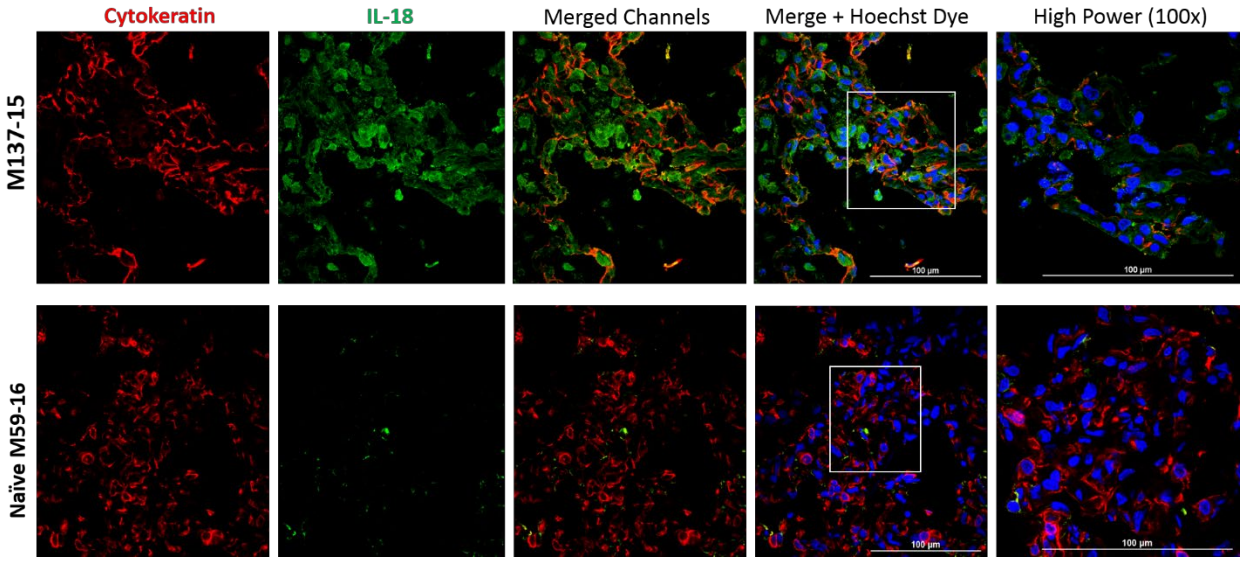

Figure 14. Cytokeratin and IL-18 Immunoflourescent Staining in situ

Infected and naïve necropsied snap frozen deep lung tissues stained for monoclonal CD163, to mark alveolar macrophages, and monoclonal IL-18. Cytokeratin was stained secondarily with Alexa fluor 546, and appears red in coloration. IL-18 was stained secondarily with Alexa fluor 488, and appears green in coloration. Hoechst dye was used to identify nuclei in cells. Scale bars, 100 µm.

In dual stains with cytokeratin and IL-18 some co-localization was observed (Figure 14). Staining within epithelial cell cytosol suggested cytokine production, as seen with the green staining. This data suggests that alveolar epithelial cells are the source of IL-18 cytokine signaling in lungs during influenza, and recruit neutrophils to the site of infection.

5.2.2 NETosis of Neutrophils Within Deep Lung Tissue

To identify NETosis within virus-challenged tissues, dual immunoflourescent stains for antibodies to both H3 histones and either influenza A nucleoprotein or active IL-1β were used. An H3 histone antibody marker was used to identify citrullinated histones, as nucleoprotein from NETs is citrullinated when produced through vital or suicidal NETosis. Infected tissues with both influenza A nucleoprotein dual stains and IL-1β dual staining showed high expressions of H3

histone NETs within deep lung tissue, compared to naive tissue sections (Figures 15 and 16). More specifically, influenza A nucleoprotein corrleated with potentially infected neutrophils and seen in areas of high H3 expression (Figure 15). As well, areas of H3 staining had high expression of IL-1β cytokine when compared to naïve tissues (Figure 15). Co-localization of influenza A nucleoprotein and H3 histones suggests infected neutrophils in the deep lung and NETosis during viral challenge. Pro-inflammatory IL-1β co-localized with H3 histones exemplifies the pro-inflammatory nature of NETosis. These sites of infection with pro-inflammatory signaling and H3 citrullinated histones from alveolar or recruited neutrophils, suggest the presence of NETosis during disease progression.

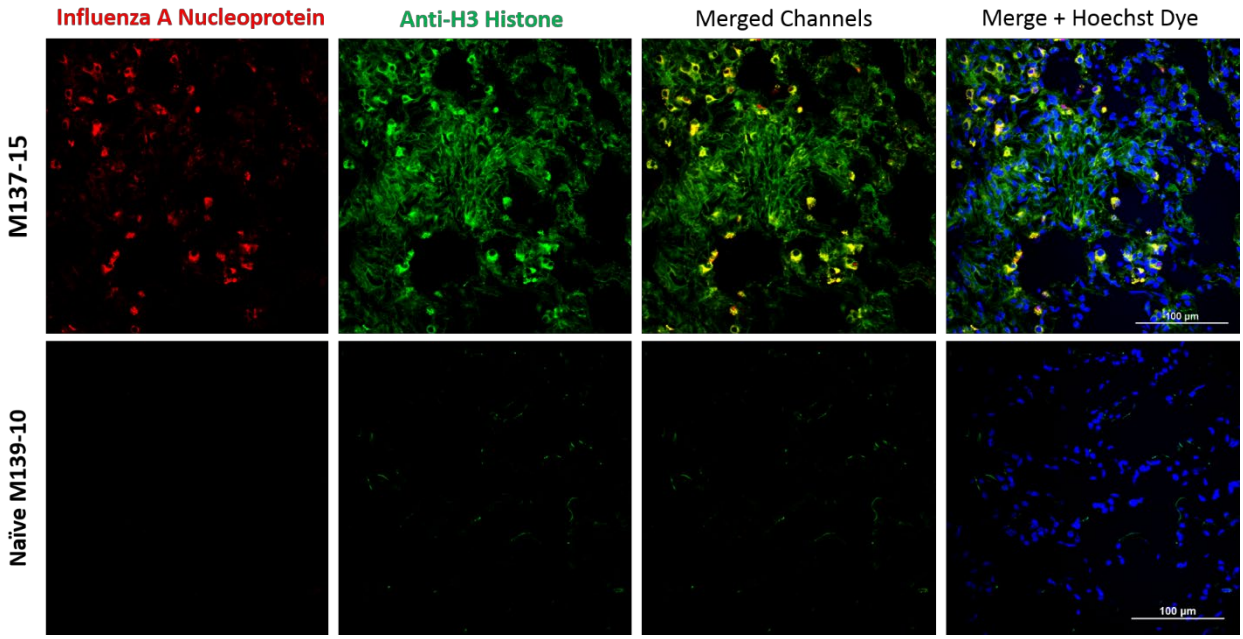

Figure 15. Influenza A Nuceloprotein and Anti-H3 Histone Immunoflourescent Staining in situ

Infected and naïve necropsied snap frozen deep lung tissues stained for monoclonal influenza A nucleoprotein and monoclonal anti-H3 Histone. Influenza A nucleoprotein was stained secondarily with Alexa fluor 546, and appears red in coloration. Anti-h3 histone was stained secondarily with Alexa fluor 488, and appear green in coloration. Hoechst dye was used to identify nuclei in cells. Scale bars, 100 µm.

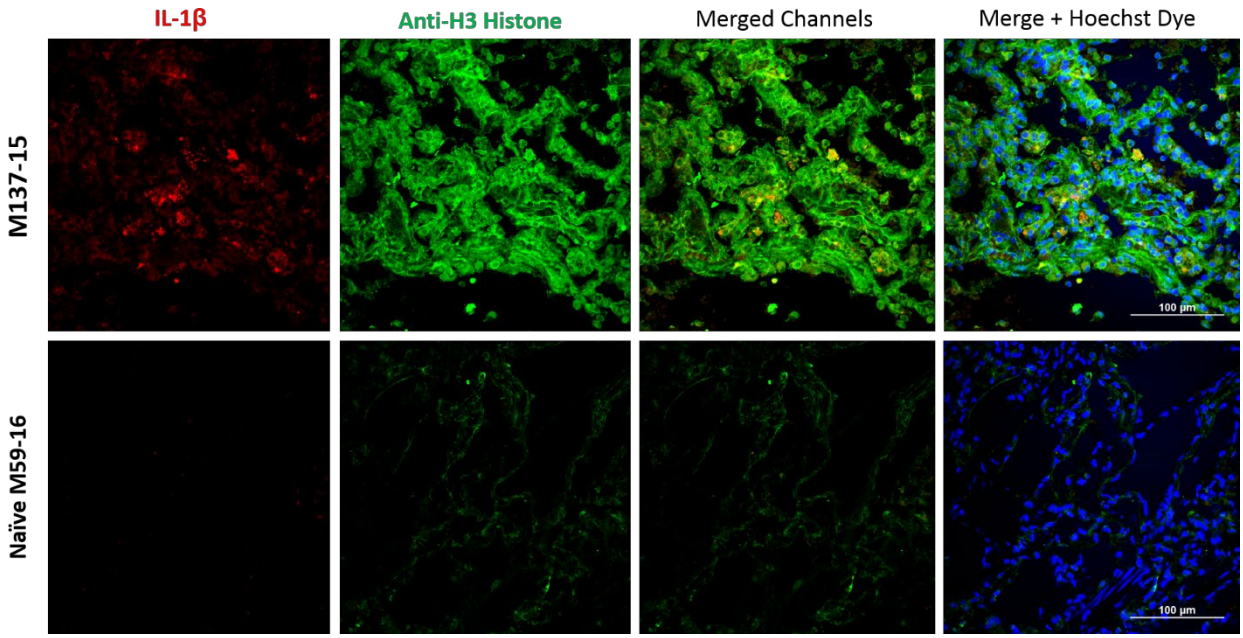

Figure 16. IL-1β and Anti-H3 Histone Immunoflourescent Staining in situ

Infected and naïve necropsied snap frozen deep lung tissues stained for monoclonal influenza A nucleoprotein and monoclonal anti-H3 Histone. IL-1β was stained secondarily with Alexa fluor 647, and appears red in coloration. Anti-h3 histone was stained secondarily with Alexa fluor 488, and appear green in coloration. Hoechst dye was used to identify nuclei in cells. Scale bars, 100 µm.

After observing high expression of H3 Histone NETs in infected tissues, images were recaptured and utilized in quantitaitve analysis via Nis Elements. Compared to naïve tissues, citrullinated h3 histones were significantly increased in post-infected tissue sections (Figure 17). When analyzing co-localization of IL-1β with H3 histones in post-infected tissue slides, no difference between H3 co-localized with IL-1β and IL-1β by itself was found(Figure 18). These data suggest that compared to naïve tissue, NETosis is highly expressed in infected tissue. It appears that although previous studies have shown the pro-inflammatory nature of NETs, there is not a significant increase in IL-1β expression from infected area with high NET expression.

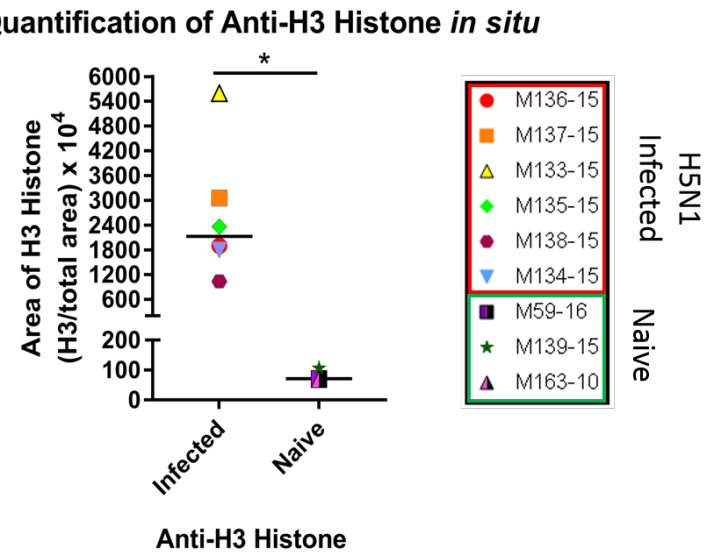

Figure 17. Quantification of Anti-H3 Histone

A) Quantification of anti-H3 Histone within necropsied snap frozen tissues from post-infected and naïve animals dual stained with anti-H3 Histone and IL-1β. The *p* values were determined through Mann-Whitney U tests. *$p < 0.05$.

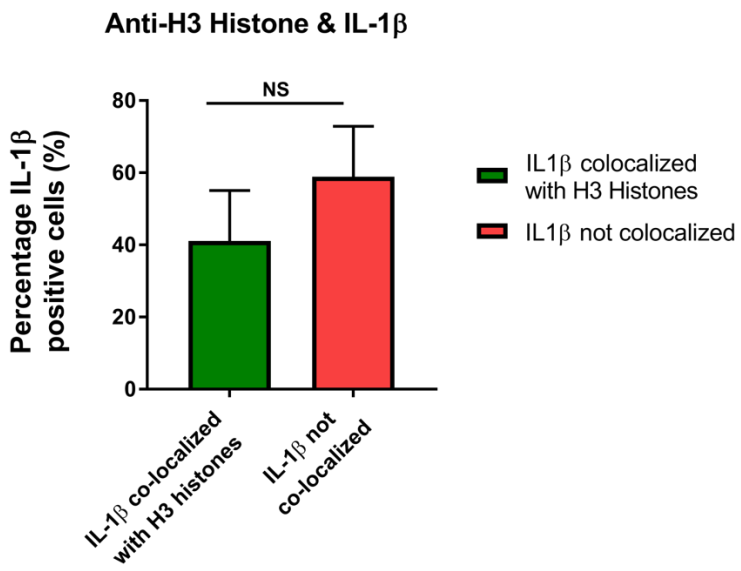

Figure 18. Quantification of Co-localization of Anti-H3 Histone and IL-1β

Quantification of co-localization of anti-H3 histone with IL-1β. The *p* values were determined through Mann-Whitney U tests. *$p < 0.05$.

5.2.3 Aim 2 Conclusions

In aim 2, I found that IL-18 co-localized with cytokeratin, our marker for epithelial cells, suggesting that alveolar epithelial cells generate neutrophil cytokine signaling in infected tissues. A high expression of H3 histones in infected tissues suggest that NETosis of neutrophils is occurring in lungs infected with H5N1. Finally, NETosis and IL-1β co-localization suggest pro-inflammatory cytokine expression in area that express NETs or affirms the IL-1β generation from NETs located in the ECM.

5.3 Aim 3

While the data in the previous aims does point to active capase-1 and NETs within the lower respiratory tract of animals, the data does not relate directly to disease severity after aerosol challenge. To determine if animals exposed to H5N1 influenza aerosol had disease severity related to caspase-1 and NETs expression we examined previous recorded data from the study completed by Wonderlich et. al [11]. As part of this previous study, all animals who were challenged via H5N1 influenza aerosol also underwent molecular imaging via fludeoxyglucose positron emission tomography-computer tomography (FDG PET-CT) [11]. FDG is a radiotracer used to measure cellular activity, and when used with PET-CT you are able to visualize cell activity associated with tomography of the site of infection, for instance measuring cellular inflammation from H5N1 influenza infection in the lower respiratory track. In addition, animals in the infected group also had concentrations of albumin measured from BAL fluids. Albumin levels in the previous study were analyzed to determine if alveolar epithelial cell death was a contributing factor to fluid leakage after ARDs development from disease progression [11].

To identify if caspase-1 and NETs are associated with disease progression or severity, quantitative analysis of the data collected from the previous study and the data collected during this study was completed.

5.3.1 Caspase-1 and NETs in Clinical Disease

When correlating caspase-1 with FDG PET-CT, we found a positive correlation with a p value of 0.0167 (Figure 19). Similarly, we found a positive correlation with NETs expression and high inflammation levels measured through FDG PET-CT (Figure 19). As stated above,

FDG PET-CT is a measure of cellular activity related to tomography at the site of infection. In the previous study, FDG PET-CT was used to cell inflammatory responses after aerosol challenge [11]. Both of the positive correlations above, point to caspase-1 and NETs being directly associated with inflammation from H5N1 HPAI aerosol challenge and disease severity.

When comparing albumin levels collected from BAL completed in our infected animal group, neither caspase-1 or NETs correlated positively with an increase in albumin levels (Figure 20). As stated previously, alveolar epithelial cell death was suggested to contribute to fluid leakage in the alveolar space and lead to ARDs in cynomologus macaques. As shown in the previous study, increased albumin levels were found in BAL fluid from cynomologus macaques infected with H5N1 [11]. However correlate data presented in this study, suggests that caspase-1 and NETs do not have a direct association with fluid presentation from H5N1 influenza disease progression, and may not be contributing to fluid accumulation after alveolar cell death.

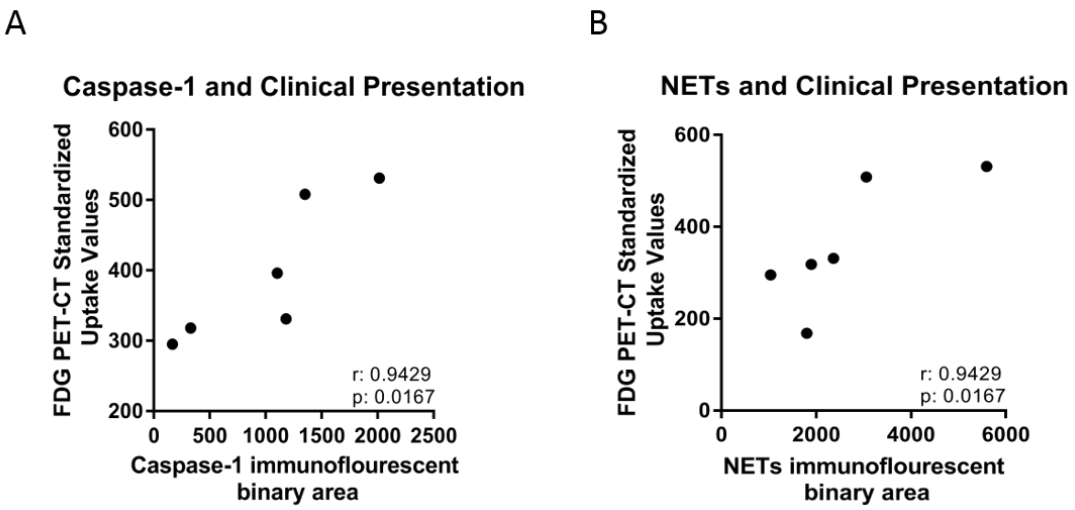

Figure 19. Caspase-1 and NETs in Clinical disease
Caspase-1 binary areas from immunoflourescent staining *in situ* plotted against FDG PET-CT standardized uptake values. Fludeoxyglucose (FDG) PET-CT is used to identify areas of high cellular activity, marking inflammation at sites of infection. Caspase-1 is used as a marker for caspase-1 mediated pro-inflammatory cytokine pathways. B) NETs binary areas from immunoflourescent staining *in situ* against FDG PET-CT standardized uptake values. FDG PET-CT is used to identify areas of high cellular activity, marking inflammation at sites of infection. NETs are used to identify neutrophil extracellular traps generated through NETosis. Each point presented is an individual animal that was challenged with H5N1 influenza aerosol.The p values were determined through Spearman r correlates. *p < 0.05.

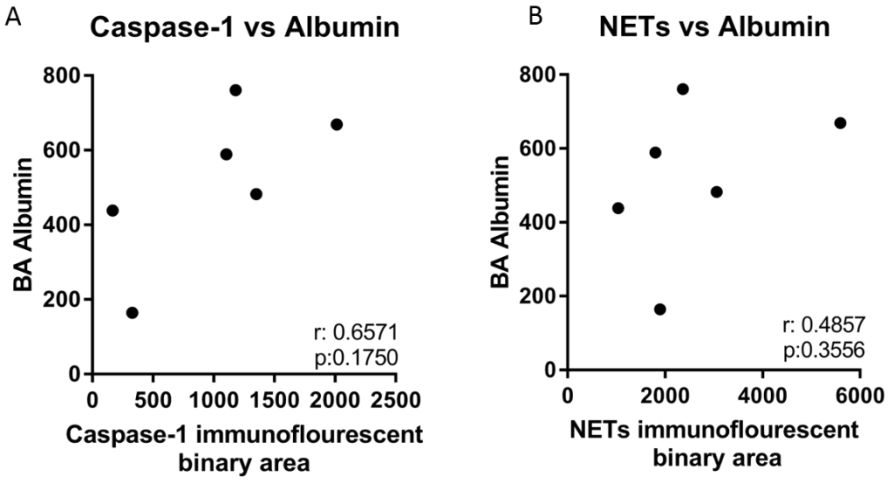

Figure 20. Caspase-1 and NETs Compared Against Albumin Levels
A) Caspase-1 binary areas from immunoflourescent staining *in situ* against albumin levels measured through BAL. B) NETs binary areas from immunoflourescent staining *in situ* against albumin levels. Each point presented is an individual animal that was challenged with H5N1 influenza aerosol. The p values were determined through Spearman r correlates. *p < 0.05.

After correlating caspase-1 and NETs with FDG PET-CT, I decided to correlate caspase-1 and NETs to see if caspase-1 expression was associated with NET expression from recruited neutrophils. A positive correlation between caspase-1 and NETs was found suggesting that area that express caspase-1 also are likely to express NETosis and that the two are associated with disease severity after H5N1 influenza aersol challenge (Figure 21).

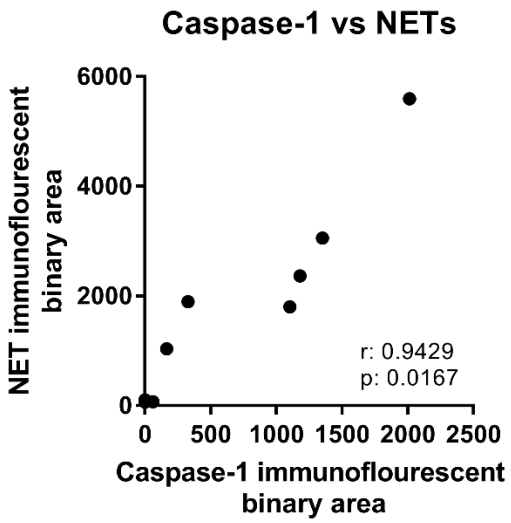

Figure 21. Caspase-1 Correlated with NETs in situ

Caspase-1 binary areas from immunoflourescent staining *in situ* correlated to NETs binary area from immonuflourescent staining *in situ*. Each point presented is an individual animal, including naive controls and the infected group. The p values were determined through Spearman r correlates. *p < 0.05.

5.3.2 Aim 3 Conclusions

At the end of aim 3, I found that caspase-1 and NET expression in infected tissues are correlated to disease severity in cynomologus macaques infected by H5N1 aerosol. I found that caspase-1 and NETs do not have direct relationships to increases in albumin found in BAL

fluids. Finally, I found that caspase-1 and NETs expressed in infected tissues are correlated. This correlation suggest that caspase-1 pro-inflammatory cytokine generation leads to cytokine recruitment of neutrophils who undergo NETosis in H5N1 infected tissues.

6.0 Discussion

In previous studies, severe disease progression during H5N1 highly pathogenic avian influenza has been shown to increase pro-inflammatory cytokines within the lower respiratory tract and systemically through the body in both humans and non-human primates [11, 21, 101]. Further clarifcation of disease mechanisms at a cellular level is required to better understand viral infection. Previous groups have elucidated the effect of viral challenge at a cellular level within the lung and have found apoptotoic cell death of pneumocytes and alveolar epithelial cells within both human and non-human primate samples [102, 103]. While apoptotic cell death may occur in infected lung tissues, this fails to explain the high expression of cytokines within the lung. Apoptotic cell death also fails to explain the large amount of fluid present, leading to secondary fulminant pneumonia in both cynamolgus macques and human infected with H5N1. Furthermore, previous studies involving H5N1 influenza do not fully recapitulate natural course of disease as most introduce viral challenge via intra-tracheal liquid suspension alongside inoculum to the eyes, nose, or mouth. Tissue samples collected from a previous study, Wonderlich et. al, and used in this study were instead challenged via aeroslized H5N1 and show disease progression more akin to natural course of disease in human cases[11]. Aerosol infection has also demonstrated high pro-inflammatory cytokines expression, similar to natural disease progression, and mean death times are comparable to those seen in natural infection.

With study data from the previous study more akin to natural infection, I expected to see pro-inflammatory cytokine expression to be much higher in infected tissues rather than naïve

tissues. Not only did I find high expression of pro-inflammatory cytokines, but as well I found them to be correlated to influenza A nucleoprotein and to inflammasome related protein ASC. Quantitative and qualitative analysis of in situ immunoflourescent staining show high titers of caspase-1, IL-1β, and IL-18 as expected. These pro-inflammatory cytokines are all associated with caspase-1 mediated pro-inflammatory cytokine pathway. High concentrations of ASC protein within the tissues along with caspase-1 mediated cytokine expression suggest pyroptotic cellular disease progression within deep lung, most likely occuring within infected alveolar epithelial cells. Data from this study strengthens findings of pyroptotic cellular death driven by caspase-1, either simultaneously occuring with or insead of apoptotic cellular death. Ultimately these data point to caspase-1 mediated disease progression, and pro-inflammatory pyroptotic cell death of alevolar epithelial cells after viral challenge.

As suggested in Webster et. al, inhibition of cytokine production within H5N1 infected mice did not prevent or protect mice from death during lethal influenza challenge [111]. The study tested TNF-α, IL-6, CCL2, and glucocorticoids within mice and looked for differentiation between genetically deficient mice for these cytokines and steroids. While TNF-α, IL-6, CCL2, and glucocorticoids are important in disease progression, within their study they do not seem to have a generative effect for disease. In Wonderlich et. al, pro-inflammatory cytokine expression was dramatically increased in non-human primates challenged with aersolized H5N1, especially titers of IL-1β found in both tissues and bronchoalveolar lavages (BALs) [11]. With the data presented via this study, I expected to see high titers of IL-1β expressed in situ of H5N1 post-infected cyanomolgus macques. As the data demonstrate, not only do infected animals exhibit high titers of IL-1β, but they also exhibit its effector cytokine, caspase-1, and Il-18. This data suggests that pro-inflammatory cytokines are abundant in disease, and may be an essential part of disease progression. Furthermore, the data suggests that caspase-1 mediated disease progression may be a driving force for severe influenza after viral challenge.

High expression of IL-18 as seen in a previous study done by Wonderlich et. al, has been hypothesized to be a recruitment signal for neutrophils to the site of infection [11]. I expected that *in situ* staining of infected tissues would affirm high concentrations of Il-18. As the data suggest IL-18 in addition to other cytokines from the caspase-1 mediated pro-inflammaotry cytokine pathway are highly expressed in post infected tissues. This data suggests that IL-18 signaling from alveolar epithelial cells recruits neutrophils to the site of infection after aerosol challenge. Furthermore, large populations of neutrophils and macrophages were found in infected tissue, affirming the results of high populations found in BALs and tissues from Wonderlich et. al [11].

As suggested in Wonderlich et. al, after H5N1 influenza infection there is a large recruitment of neutrophils to the site of infection [11]. Narasaraju et. al found not only large recruitment of neutrophils in severe season influenza A infection, but NETosis within alevolar spaces attributing to complications during secondary pneumococcal infection [112]. As a result, I expected to see an increase in neutrophil numbers and NETS within infected tissue as compared to naïve tissue sections. As the data suggest, not only is there a large number of neutrophils at the site of infection, but there is also large amount of expressed citrullinated H3 histone in relation to vital or suicidal NETosis. The staining and quantitative data show a statistically significant increase in citrullinated h3 histone associated with NETs. NETs within H5N1 infected samples demostrate NETosis during primary viral disease progression and or during sceondary infection of pneumoncoccal bacteria leading to fulminant pneumonia. Furthermore, *in situ* immunoflourecence demonstrates alveolar tissue inflammation and leaking of interstitial fluid in to alveolar spaces. The data suggests presentation of NETs within the deep lung that trap both viral particulate and bacteria, as well as fluids from leakage of interstitum after tearing of alveolar tissue. This “double edged sword” action may exacerbate disease,

cause hyperventilation, and decrease tidal volumes as seen in Wonderlich et. al after aerosolized viral challenge.

As a final part to this study I wished to correlated disease severity with presentation of caspase-1 and NETs within lower respiratory tract tissue. As the data suggests the animals infected via aerosol exposure, in the study completed by Wonderlich et. al, have high correlates of disease severity with both caspase-1 and NETosis [11]. This affirms the notion that caspase-1 mediated disease cooperates with severe disease progression alognside NETosis of neutrophils recruited to the site of infection. In addition, the data suggests that areas of infection with high NETosis also present high levels of pro-inflammatory caspase-1. All together the data suggests that caspase-1 and NETosis develop as a result of severe disease progression and may be targets for furture therapeutic treatments.

A prime limitation of this study is the power associated with the statistical analysis performed on the quatitative imaging. The number of tissue samples available for study were limited and the variation in disease progression across animals did not distribute evenly. As a result instead of individual day time point analysis, groups of infected and naïve tissue were used. In addition the number of images taken for each tissue was lower than expected due to the limited number of tissues available for sectioning. Further experimentation on live animal models and *ex vivo* samples, as well as more image analysis would be beneficial to confirm statistically significant increases in cytokine expression and NETS expression when comparing post-infected and naïve groups.

Overall this data suggest the expression of caspase-1 mediated pro-inflammatory cytokine pathways after H5N1 viral infection, in additon to the development of NETs from alveolar and recruited neutrophils after H5N1 viral infection. Identification of caspase-1 mediated disease progression and NETs within deep lung tissue of non-human primates infected with H5N1 highly pathogenic avian influenza allows for clarification of cellular disease

mechanism. Additionally, identification of these cellular disease mechanisms can act as potential targets for therapeutics.

Currently HPAI A infection preparedness revolves around active vaccination of both farm workers who handle domestic avian populations, and active vaccination of vectors who have the potential to be infected including domestic and wild fowl [113]. Although benefical, this leaves a large gap in preparedness especially regarding an animal cross-over event of a highly pathogenic influenza A virus. A cross over event of a novel highly pathogenic avian influenza strain could lead to pandemic scale infection and is highly detrimental to public health efforts. Therapeutic and cure research in H5N1 and other types of highly pathogenic influenza A viruses is therefore a necessity. Introduction of novel therapeutics could assist in limiting the number of fatal cases of H5N1 highly pathogenic avian influenza and reduce the case fatality ratio found from previous infection of both cynomologus macaques and human cases. While this data is only a start towards novel therapeutics, cure and therapeutic research must proceed alongside cellular disease mechanisms in order to prevent H5N1 highly pathogenic avian influenza cross over events and to further benefit public health research.

7.0 Future Work

While the data presented suggest caspase-1 mediated pro-inflammatory cytokine pathways within deep lung after viral challenge further research into cellular mechanisms is still required. In order to determine pyroptotic cell death within tissue, experiments identifying active gasdermin d, the pore forming complex in pyroptotic cell death, must be completed. Further work into the therapeutic benefits of caspase-1 inhibition could lead to novel therapeutics. In addition, research into the effects of DNAse on clearance of NETs within the deep lung in a live model could prove to be beneficial as a therapeutic treatment. Finally identification of active inflammasome complexes within the deep lung that interact with ASC, or further identification of ASC pyroptosomes within deep lung tissue could prove to be useful in finding potential site for cure or therapeutic research. Full elucidation of cellular mechanisms of disease can prove beneficial to both therapuetic and cure research, as well as assist in understanding other types of severe pulmonary viral infections.

Bibliography

1. Neumann, G., H. Chen, G.F. Gao, Y. Shu, and Y. Kawaoka, *H5N1 influenza viruses: outbreaks and biological properties.* Cell Res, 2010. **20**(1): p. 51-61.
2. Writing Committee of the Second World Health Organization Consultation on Clinical Aspects of Human Infection with Avian Influenza, A.V., A.N. Abdel-Ghafar, T. Chotpitayasunondh, Z. Gao, F.G. Hayden, D.H. Nguyen, M.D. de Jong, A. Naghdaliyev, J.S. Peiris, N. Shindo, S. Soeroso, and T.M. Uyeki, *Update on avian influenza A (H5N1) virus infection in humans.* N Engl J Med, 2008. **358**(3): p. 261-73.
3. Matrosovich, M.N., T.Y. Matrosovich, T. Gray, N.A. Roberts, and H.D. Klenk, *Human and avian influenza viruses target different cell types in cultures of human airway epithelium.* Proc Natl Acad Sci U S A, 2004. **101**(13): p. 4620-4.
4. Nicholls, J.M., M.C. Chan, W.Y. Chan, H.K. Wong, C.Y. Cheung, D.L. Kwong, M.P. Wong, W.H. Chui, L.L. Poon, S.W. Tsao, Y. Guan, and J.S. Peiris, *Tropism of avian influenza A (H5N1) in the upper and lower respiratory tract.* Nat Med, 2007. **13**(2): p. 147-9.
5. van Riel, D., V.J. Munster, E. de Wit, G.F. Rimmelzwaan, R.A. Fouchier, A.D. Osterhaus, and T. Kuiken, *H5N1 Virus Attachment to Lower Respiratory Tract.* Science, 2006. **312**(5772): p. 399.
6. Subbarao, K., A. Klimov, J. Katz, H. Regnery, W. Lim, H. Hall, M. Perdue, D. Swayne, C. Bender, J. Huang, M. Hemphill, T. Rowe, M. Shaw, X. Xu, K. Fukuda, and N. Cox, *Characterization of an avian influenza A (H5N1) virus isolated from a child with a fatal respiratory illness.* Science, 1998. **279**(5349): p. 393-6.
7. Claas, E.C., J.C. de Jong, R. van Beek, G.F. Rimmelzwaan, and A.D. Osterhaus, *Human influenza virus A/HongKong/156/97 (H5N1) infection.* Vaccine, 1998. **16**(9-10): p. 977-8.
8. Peiris, J.S., W.C. Yu, C.W. Leung, C.Y. Cheung, W.F. Ng, J.M. Nicholls, T.K. Ng, K.H. Chan, S.T. Lai, W.L. Lim, K.Y. Yuen, and Y. Guan, *Re-emergence of fatal human influenza A subtype H5N1 disease.* Lancet, 2004. **363**(9409): p. 617-9.
9. Barnard, D.L., *Animal models for the study of influenza pathogenesis and therapy.* Antiviral Res, 2009. **82**(2): p. A110-22.
10. Lakdawala, S.S., A. Jayaraman, R.A. Halpin, E.W. Lamirande, A.R. Shih, T.B. Stockwell, X. Lin, A. Simenauer, C.T. Hanson, L. Vogel, M. Paskel, M. Minai, I. Moore, M. Orandle, S.R. Das, D.E. Wentworth, R. Sasisekharan, and K. Subbarao, *The soft palate is an important site of adaptation for transmissible influenza viruses.* Nature, 2015. **526**(7571): p. 122-5.
11. Wonderlich, E.R., Z.D. Swan, S.J. Bissel, A.L. Hartman, J.P. Carney, K.J. O'Malley, A.O. Obadan, J. Santos, R. Walker, T.J. Sturgeon, L.J. Frye, Jr., P. Maiello, C.A. Scanga, J.D. Bowling, A.L. Bouwer, P.A. Duangkhae, C.A. Wiley, J.L. Flynn, J. Wang, K.S. Cole, D.R. Perez, D.S. Reed, and S.M. Barratt-Boyes, *Widespread Virus Replication in Alveoli Drives Acute Respiratory Distress Syndrome in Aerosolized H5N1 Influenza Infection of Macaques.* J Immunol, 2017. **198**(4): p. 1616-1626.
12. Short, K.R., E. Kroeze, R.A.M. Fouchier, and T. Kuiken, *Pathogenesis of influenza-induced acute respiratory distress syndrome.* Lancet Infect Dis, 2014. **14**(1): p. 57-69.
13. Baskin, C.R., H. Bielefeldt-Ohmann, T.M. Tumpey, P.J. Sabourin, J.P. Long, A. Garcia-Sastre, A.E. Tolnay, R. Albrecht, J.A. Pyles, P.H. Olson, L.D. Aicher, E.R. Rosenzweig,

K. Murali-Krishna, E.A. Clark, M.S. Kotur, J.L. Fornek, S. Proll, R.E. Palermo, C.L. Sabourin, and M.G. Katze, *Early and sustained innate immune response defines pathology and death in nonhuman primates infected by highly pathogenic influenza virus.* Proc Natl Acad Sci U S A, 2009. **106**(9): p. 3455-60.
14. Cilloniz, C., K. Shinya, X. Peng, M.J. Korth, S.C. Proll, L.D. Aicher, V.S. Carter, J.H. Chang, D. Kobasa, F. Feldmann, J.E. Strong, H. Feldmann, Y. Kawaoka, and M.G. Katze, *Lethal influenza virus infection in macaques is associated with early dysregulation of inflammatory related genes.* PLoS Pathog, 2009. **5**(10): p. e1000604.
15. Shinya, K., Y. Gao, C. Cilloniz, Y. Suzuki, M. Fujie, G. Deng, Q. Zhu, S. Fan, A. Makino, Y. Muramoto, S. Fukuyama, D. Tamura, T. Noda, A.J. Eisfeld, M.G. Katze, H. Chen, and Y. Kawaoka, *Integrated clinical, pathologic, virologic, and transcriptomic analysis of H5N1 influenza virus-induced viral pneumonia in the rhesus macaque.* J Virol, 2012. **86**(11): p. 6055-66.
16. Fujiyuki, T., M. Yoneda, F. Yasui, T. Kuraishi, S. Hattori, H.J. Kwon, K. Munekata, Y. Kiso, H. Kida, M. Kohara, and C. Kai, *Experimental infection of macaques with a wild water bird-derived highly pathogenic avian influenza virus (H5N1).* PLoS One, 2013. **8**(12): p. e83551.
17. Muramoto, Y., J.E. Shoemaker, M.Q. Le, Y. Itoh, D. Tamura, Y. Sakai-Tagawa, H. Imai, R. Uraki, R. Takano, E. Kawakami, M. Ito, K. Okamoto, H. Ishigaki, H. Mimuro, C. Sasakawa, Y. Matsuoka, T. Noda, S. Fukuyama, K. Ogasawara, H. Kitano, and Y. Kawaoka, *Disease severity is associated with differential gene expression at the early and late phases of infection in nonhuman primates infected with different H5N1 highly pathogenic avian influenza viruses.* J Virol, 2014. **88**(16): p. 8981-97.
18. Rimmelzwaan, G.F., T. Kuiken, G. van Amerongen, T.M. Bestebroer, R.A. Fouchier, and A.D. Osterhaus, *Pathogenesis of influenza A (H5N1) virus infection in a primate model.* J Virol, 2001. **75**(14): p. 6687-91.
19. Soloff, A.C., S.J. Bissel, B.F. Junecko, B.M. Giles, T.A. Reinhart, T.M. Ross, and S.M. Barratt-Boyes, *Massive mobilization of dendritic cells during influenza A virus subtype H5N1 infection of nonhuman primates.* J Infect Dis, 2014. **209**(12): p. 2012-6.
20. Chan, M.C., C.Y. Cheung, W.H. Chui, S.W. Tsao, J.M. Nicholls, Y.O. Chan, R.W. Chan, H.T. Long, L.L. Poon, Y. Guan, and J.S. Peiris, *Proinflammatory cytokine responses induced by influenza A (H5N1) viruses in primary human alveolar and bronchial epithelial cells.* Respir Res, 2005. **6**: p. 135.
21. Cheung, C.Y., L.L. Poon, A.S. Lau, W. Luk, Y.L. Lau, K.F. Shortridge, S. Gordon, Y. Guan, and J.S. Peiris, *Induction of proinflammatory cytokines in human macrophages by influenza A (H5N1) viruses: a mechanism for the unusual severity of human disease?* Lancet, 2002. **360**(9348): p. 1831-7.
22. Schroder, K. and J. Tschopp, *The inflammasomes.* Cell, 2010. **140**(6): p. 821-32.
23. Guo, H., J.B. Callaway, and J.P. Ting, *Inflammasomes: mechanism of action, role in disease, and therapeutics.* Nat Med, 2015. **21**(7): p. 677-87.
24. Bergsbaken, T., S.L. Fink, and B.T. Cookson, *Pyroptosis: host cell death and inflammation.* Nat Rev Microbiol, 2009. **7**(2): p. 99-109.
25. Man, S.M. and T.D. Kanneganti, *Converging roles of caspases in inflammasome activation, cell death and innate immunity.* Nat Rev Immunol, 2016. **16**(1): p. 7-21.
26. Broz, P. and V.M. Dixit, *Inflammasomes: mechanism of assembly, regulation and signalling.* Nat Rev Immunol, 2016. **16**(7): p. 407-20.
27. Miao, E.A., J.V. Rajan, and A. Aderem, *Caspase-1-induced pyroptotic cell death.* Immunol Rev, 2011. **243**(1): p. 206-14.
28. Fraser, J.R., T.C. Laurent, and U.B. Laurent, *Hyaluronan: its nature, distribution, functions and turnover.* J Intern Med, 1997. **242**(1): p. 27-33.
29. Laurent, T.C., *Biochemistry of hyaluronan.* Acta Otolaryngol Suppl, 1987. **442**: p. 7-24.

30. Sagulenko, V., S.J. Thygesen, D.P. Sester, A. Idris, J.A. Cridland, P.R. Vajjhala, T.L. Roberts, K. Schroder, J.E. Vince, J.M. Hill, J. Silke, and K.J. Stacey, *AIM2 and NLRP3 inflammasomes activate both apoptotic and pyroptotic death pathways via ASC.* Cell Death Differ, 2013. **20**(9): p. 1149-60.
31. Fernandes-Alnemri, T., J. Wu, J.W. Yu, P. Datta, B. Miller, W. Jankowski, S. Rosenberg, J. Zhang, and E.S. Alnemri, *The pyroptosome: a supramolecular assembly of ASC dimers mediating inflammatory cell death via caspase-1 activation.* Cell Death Differ, 2007. **14**(9): p. 1590-604.
32. Bryan, N.B., A. Dorfleutner, S.J. Kramer, C. Yun, Y. Rojanasakul, and C. Stehlik, *Differential splicing of the apoptosis-associated speck like protein containing a caspase recruitment domain (ASC) regulates inflammasomes.* J Inflamm (Lond), 2010. **7**: p. 23.
33. Galluzzi, L., I. Vitale, S.A. Aaronson, J.M. Abrams, D. Adam, P. Agostinis, E.S. Alnemri, L. Altucci, I. Amelio, D.W. Andrews, M. Annicchiarico-Petruzzelli, A.V. Antonov, E. Arama, E.H. Baehrecke, N.A. Barlev, N.G. Bazan, F. Bernassola, M.J.M. Bertrand, K. Bianchi, M.V. Blagosklonny, K. Blomgren, C. Borner, P. Boya, C. Brenner, M. Campanella, E. Candi, D. Carmona-Gutierrez, F. Cecconi, F.K. Chan, N.S. Chandel, E.H. Cheng, J.E. Chipuk, J.A. Cidlowski, A. Ciechanover, G.M. Cohen, M. Conrad, J.R. Cubillos-Ruiz, P.E. Czabotar, V. D'Angiolella, T.M. Dawson, V.L. Dawson, V. De Laurenzi, R. De Maria, K.M. Debatin, R.J. DeBerardinis, M. Deshmukh, N. Di Daniele, F. Di Virgilio, V.M. Dixit, S.J. Dixon, C.S. Duckett, B.D. Dynlacht, W.S. El-Deiry, J.W. Elrod, G.M. Fimia, S. Fulda, A.J. Garcia-Saez, A.D. Garg, C. Garrido, E. Gavathiotis, P. Golstein, E. Gottlieb, D.R. Green, L.A. Greene, H. Gronemeyer, A. Gross, G. Hajnoczky, J.M. Hardwick, I.S. Harris, M.O. Hengartner, C. Hetz, H. Ichijo, M. Jaattela, B. Joseph, P.J. Jost, P.P. Juin, W.J. Kaiser, M. Karin, T. Kaufmann, O. Kepp, A. Kimchi, R.N. Kitsis, D.J. Klionsky, R.A. Knight, S. Kumar, S.W. Lee, J.J. Lemasters, B. Levine, A. Linkermann, S.A. Lipton, R.A. Lockshin, C. Lopez-Otin, S.W. Lowe, T. Luedde, E. Lugli, M. MacFarlane, F. Madeo, M. Malewicz, W. Malorni, G. Manic, J.C. Marine, S.J. Martin, J.C. Martinou, J.P. Medema, P. Mehlen, P. Meier, S. Melino, E.A. Miao, J.D. Molkentin, U.M. Moll, C. Munoz-Pinedo, S. Nagata, G. Nunez, A. Oberst, M. Oren, M. Overholtzer, M. Pagano, T. Panaretakis, M. Pasparakis, J.M. Penninger, D.M. Pereira, S. Pervaiz, M.E. Peter, M. Piacentini, P. Pinton, J.H.M. Prehn, H. Puthalakath, G.A. Rabinovich, M. Rehm, R. Rizzuto, C.M.P. Rodrigues, D.C. Rubinsztein, T. Rudel, K.M. Ryan, E. Sayan, L. Scorrano, F. Shao, Y. Shi, J. Silke, H.U. Simon, A. Sistigu, B.R. Stockwell, A. Strasser, G. Szabadkai, S.W.G. Tait, D. Tang, N. Tavernarakis, A. Thorburn, Y. Tsujimoto, B. Turk, T. Vanden Berghe, P. Vandenabeele, M.G. Vander Heiden, A. Villunger, H.W. Virgin, K.H. Vousden, D. Vucic, E.F. Wagner, H. Walczak, D. Wallach, Y. Wang, J.A. Wells, W. Wood, J. Yuan, Z. Zakeri, B. Zhivotovsky, L. Zitvogel, G. Melino and G. Kroemer, *Molecular mechanisms of cell death: recommendations of the Nomenclature Committee on Cell Death 2018.* Cell Death Differ, 2018. **25**(3): p. 486-541.
34. Tait, S.W. and D.R. Green, *Mitochondria and cell death: outer membrane permeabilization and beyond.* Nat Rev Mol Cell Biol, 2010. **11**(9): p. 621-32.
35. Moldoveanu, T., A.V. Follis, R.W. Kriwacki, and D.R. Green, *Many players in BCL-2 family affairs.* Trends Biochem Sci, 2014. **39**(3): p. 101-11.
36. Edlich, F., S. Banerjee, M. Suzuki, M.M. Cleland, D. Arnoult, C. Wang, A. Neutzner, N. Tjandra, and R.J. Youle, *Bcl-x(L) retrotranslocates Bax from the mitochondria into the cytosol.* Cell, 2011. **145**(1): p. 104-16.
37. Garner, T.P., D.E. Reyna, A. Priyadarshi, H.C. Chen, S. Li, Y. Wu, Y.T. Ganesan, V.N. Malashkevich, E.H. Cheng, and E. Gavathiotis, *An Autoinhibited Dimeric Form of BAX Regulates the BAX Activation Pathway.* Mol Cell, 2016. **64**(2): p. 431.

38. Chen, H.C., M. Kanai, A. Inoue-Yamauchi, H.C. Tu, Y. Huang, D. Ren, H. Kim, S. Takeda, D.E. Reyna, P.M. Chan, Y.T. Ganesan, C.P. Liao, E. Gavathiotis, J.J. Hsieh, and E.H. Cheng, *An interconnected hierarchical model of cell death regulation by the BCL-2 family.* Nat Cell Biol, 2015. **17**(10): p. 1270-81.
39. Brouwer, J.M., D. Westphal, G. Dewson, A.Y. Robin, R.T. Uren, R. Bartolo, G.V. Thompson, P.M. Colman, R.M. Kluck, and P.E. Czabotar, *Bak core and latch domains separate during activation, and freed core domains form symmetric homodimers.* Mol Cell, 2014. **55**(6): p. 938-946.
40. Salvador-Gallego, R., M. Mund, K. Cosentino, J. Schneider, J. Unsay, U. Schraermeyer, J. Engelhardt, J. Ries, and A.J. Garcia-Saez, *Bax assembly into rings and arcs in apoptotic mitochondria is linked to membrane pores.* EMBO J, 2016. **35**(4): p. 389-401.
41. Galluzzi, L., O. Kepp, C. Trojel-Hansen, and G. Kroemer, *Non-apoptotic functions of apoptosis-regulatory proteins.* EMBO Rep, 2012. **13**(4): p. 322-30.
42. Chai, J., C. Du, J.W. Wu, S. Kyin, X. Wang, and Y. Shi, *Structural and biochemical basis of apoptotic activation by Smac/DIABLO.* Nature, 2000. **406**(6798): p. 855-62.
43. Shalini, S., L. Dorstyn, S. Dawar, and S. Kumar, *Old, new and emerging functions of caspases.* Cell Death Differ, 2015. **22**(4): p. 526-39.
44. Nagata, S., *DNA degradation in development and programmed cell death.* Annu Rev Immunol, 2005. **23**: p. 853-75.
45. Naito, M., K. Nagashima, T. Mashima, and T. Tsuruo, *Phosphatidylserine externalization is a downstream event of interleukin-1 beta-converting enzyme family protease activation during apoptosis.* Blood, 1997. **89**(6): p. 2060-6.
46. Eckelman, B.P., G.S. Salvesen, and F.L. Scott, *Human inhibitor of apoptosis proteins: why XIAP is the black sheep of the family.* EMBO Rep, 2006. **7**(10): p. 988-94.
47. Eckelman, B.P. and G.S. Salvesen, *The human anti-apoptotic proteins cIAP1 and cIAP2 bind but do not inhibit caspases.* J Biol Chem, 2006. **281**(6): p. 3254-60.
48. Aggarwal, B.B., S.C. Gupta, and J.H. Kim, *Historical perspectives on tumor necrosis factor and its superfamily: 25 years later, a golden journey.* Blood, 2012. **119**(3): p. 651-65.
49. Gibert, B. and P. Mehlen, *Dependence Receptors and Cancer: Addiction to Trophic Ligands.* Cancer Res, 2015. **75**(24): p. 5171-5.
50. Dickens, L.S., I.R. Powley, M.A. Hughes, and M. MacFarlane, *The 'complexities' of life and death: death receptor signalling platforms.* Exp Cell Res, 2012. **318**(11): p. 1269-77.
51. Boldin, M.P., T.M. Goncharov, Y.V. Goltsev, and D. Wallach, *Involvement of MACH, a novel MORT1/FADD-interacting protease, in Fas/APO-1- and TNF receptor-induced cell death.* Cell, 1996. **85**(6): p. 803-15.
52. Kavuri, S.M., P. Geserick, D. Berg, D.P. Dimitrova, M. Feoktistova, D. Siegmund, H. Gollnick, M. Neumann, H. Wajant, and M. Leverkus, *Cellular FLICE-inhibitory protein (cFLIP) isoforms block CD95- and TRAIL death receptor-induced gene induction irrespective of processing of caspase-8 or cFLIP in the death-inducing signaling complex.* J Biol Chem, 2011. **286**(19): p. 16631-46.
53. Hughes, M.A., I.R. Powley, R. Jukes-Jones, S. Horn, M. Feoktistova, L. Fairall, J.W. Schwabe, M. Leverkus, K. Cain, and M. MacFarlane, *Co-operative and Hierarchical Binding of c-FLIP and Caspase-8: A Unified Model Defines How c-FLIP Isoforms Differentially Control Cell Fate.* Mol Cell, 2016. **61**(6): p. 834-49.
54. Koenig, A., I.A. Buskiewicz, K.A. Fortner, J.Q. Russell, T. Asaoka, Y.W. He, R. Hakem, J.E. Eriksson, and R.C. Budd, *The c-FLIPL cleavage product p43FLIP promotes activation of extracellular signal-regulated kinase (ERK), nuclear factor kappaB (NF-kappaB), and caspase-8 and T cell survival.* J Biol Chem, 2014. **289**(2): p. 1183-91.

55. Jost, P.J., S. Grabow, D. Gray, M.D. McKenzie, U. Nachbur, D.C. Huang, P. Bouillet, H.E. Thomas, C. Borner, J. Silke, A. Strasser, and T. Kaufmann, *XIAP discriminates between type I and type II FAS-induced apoptosis.* Nature, 2009. **460**(7258): p. 1035-9.
56. Yin, X.M., K. Wang, A. Gross, Y. Zhao, S. Zinkel, B. Klocke, K.A. Roth, and S.J. Korsmeyer, *Bid-deficient mice are resistant to Fas-induced hepatocellular apoptosis.* Nature, 1999. **400**(6747): p. 886-91.
57. Gross, A., X.M. Yin, K. Wang, M.C. Wei, J. Jockel, C. Milliman, H. Erdjument-Bromage, P. Tempst, and S.J. Korsmeyer, *Caspase cleaved BID targets mitochondria and is required for cytochrome c release, while BCL-XL prevents this release but not tumor necrosis factor-R1/Fas death.* J Biol Chem, 1999. **274**(2): p. 1156-63.
58. Fischer, U., C. Stroh, and K. Schulze-Osthoff, *Unique and overlapping substrate specificities of caspase-8 and caspase-10.* Oncogene, 2006. **25**(1): p. 152-9.
59. Mehlen, P. and S. Tauszig-Delamasure, *Dependence receptors and colorectal cancer.* Gut, 2014. **63**(11): p. 1821-9.
60. Joubert, O., R. Nehme, D. Fleury, M. De Rivoyre, M. Bidet, A. Polidori, M. Ruat, B. Pucci, P. Mollat, and I. Mus-Veteau, *Functional studies of membrane-bound and purified human Hedgehog receptor Patched expressed in yeast.* Biochim Biophys Acta, 2009. **1788**(9): p. 1813-21.
61. Jorgensen, I. and E.A. Miao, *Pyroptotic cell death defends against intracellular pathogens.* Immunol Rev, 2015. **265**(1): p. 130-42.
62. Vanden Berghe, T., D. Demon, P. Bogaert, B. Vandendriessche, A. Goethals, B. Depuydt, M. Vuylsteke, R. Roelandt, E. Van Wonterghem, J. Vandenbroecke, S.M. Choi, E. Meyer, S. Krautwald, W. Declercq, N. Takahashi, A. Cauwels, and P. Vandenabeele, *Simultaneous targeting of IL-1 and IL-18 is required for protection against inflammatory and septic shock.* Am J Respir Crit Care Med, 2014. **189**(3): p. 282-91.
63. Aachoui, Y., V. Sagulenko, E.A. Miao, and K.J. Stacey, *Inflammasome-mediated pyroptotic and apoptotic cell death, and defense against infection.* Curr Opin Microbiol, 2013. **16**(3): p. 319-26.
64. He, W.T., H. Wan, L. Hu, P. Chen, X. Wang, Z. Huang, Z.H. Yang, C.Q. Zhong, and J. Han, *Gasdermin D is an executor of pyroptosis and required for interleukin-1beta secretion.* Cell Res, 2015. **25**(12): p. 1285-98.
65. Kayagaki, N., I.B. Stowe, B.L. Lee, K. O'Rourke, K. Anderson, S. Warming, T. Cuellar, B. Haley, M. Roose-Girma, Q.T. Phung, P.S. Liu, J.R. Lill, H. Li, J. Wu, S. Kummerfeld, J. Zhang, W.P. Lee, S.J. Snipas, G.S. Salvesen, L.X. Morris, L. Fitzgerald, Y. Zhang, E.M. Bertram, C.C. Goodnow, and V.M. Dixit, *Caspase-11 cleaves gasdermin D for non-canonical inflammasome signalling.* Nature, 2015. **526**(7575): p. 666-71.
66. Shi, J., Y. Zhao, K. Wang, X. Shi, Y. Wang, H. Huang, Y. Zhuang, T. Cai, F. Wang, and F. Shao, *Cleavage of GSDMD by inflammatory caspases determines pyroptotic cell death.* Nature, 2015. **526**(7575): p. 660-5.
67. Ding, J., K. Wang, W. Liu, Y. She, Q. Sun, J. Shi, H. Sun, D.C. Wang, and F. Shao, *Pore-forming activity and structural autoinhibition of the gasdermin family.* Nature, 2016. **535**(7610): p. 111-6.
68. Liu, X., Z. Zhang, J. Ruan, Y. Pan, V.G. Magupalli, H. Wu, and J. Lieberman, *Inflammasome-activated gasdermin D causes pyroptosis by forming membrane pores.* Nature, 2016. **535**(7610): p. 153-8.
69. Pillai, P.S., R.D. Molony, K. Martinod, H. Dong, I.K. Pang, M.C. Tal, A.G. Solis, P. Bielecki, S. Mohanty, M. Trentalange, R.J. Homer, R.A. Flavell, D.D. Wagner, R.R. Montgomery, A.C. Shaw, P. Staeheli, and A. Iwasaki, *Mx1 reveals innate pathways to antiviral resistance and lethal influenza disease.* Science, 2016. **352**(6284): p. 463-6.

70. Izzo, V., J.M. Bravo-San Pedro, V. Sica, G. Kroemer, and L. Galluzzi, *Mitochondrial Permeability Transition: New Findings and Persisting Uncertainties.* Trends Cell Biol, 2016. **26**(9): p. 655-67.
71. Vanden Berghe, T., A. Linkermann, S. Jouan-Lanhouet, H. Walczak, and P. Vandenabeele, *Regulated necrosis: the expanding network of non-apoptotic cell death pathways.* Nat Rev Mol Cell Biol, 2014. **15**(2): p. 135-47.
72. Baines, C.P., R.A. Kaiser, N.H. Purcell, N.S. Blair, H. Osinska, M.A. Hambleton, E.W. Brunskill, M.R. Sayen, R.A. Gottlieb, G.W. Dorn, J. Robbins, and J.D. Molkentin, *Loss of cyclophilin D reveals a critical role for mitochondrial permeability transition in cell death.* Nature, 2005. **434**(7033): p. 658-62.
73. Nakagawa, T., S. Shimizu, T. Watanabe, O. Yamaguchi, K. Otsu, H. Yamagata, H. Inohara, T. Kubo, and Y. Tsujimoto, *Cyclophilin D-dependent mitochondrial permeability transition regulates some necrotic but not apoptotic cell death.* Nature, 2005. **434**(7033): p. 652-8.
74. Schinzel, A.C., O. Takeuchi, Z. Huang, J.K. Fisher, Z. Zhou, J. Rubens, C. Hetz, N.N. Danial, M.A. Moskowitz, and S.J. Korsmeyer, *Cyclophilin D is a component of mitochondrial permeability transition and mediates neuronal cell death after focal cerebral ischemia.* Proc Natl Acad Sci U S A, 2005. **102**(34): p. 12005-10.
75. Linkermann, A. and D.R. Green, *Necroptosis.* N Engl J Med, 2014. **370**(5): p. 455-65.
76. Vercammen, D., P. Vandenabeele, R. Beyaert, W. Declercq, and W. Fiers, *Tumour necrosis factor-induced necrosis versus anti-Fas-induced apoptosis in L929 cells.* Cytokine, 1997. **9**(11): p. 801-8.
77. Kaczmarek, A., P. Vandenabeele, and D.V. Krysko, *Necroptosis: the release of damage-associated molecular patterns and its physiological relevance.* Immunity, 2013. **38**(2): p. 209-23.
78. Zhang, X., C. Fan, H. Zhang, Q. Zhao, Y. Liu, C. Xu, Q. Xie, X. Wu, X. Yu, J. Zhang, and H. Zhang, *MLKL and FADD Are Critical for Suppressing Progressive Lymphoproliferative Disease and Activating the NLRP3 Inflammasome.* Cell Rep, 2016. **16**(12): p. 3247-3259.
79. Kaiser, W.J., H. Sridharan, C. Huang, P. Mandal, J.W. Upton, P.J. Gough, C.A. Sehon, R.W. Marquis, J. Bertin, and E.S. Mocarski, *Toll-like receptor 3-mediated necrosis via TRIF, RIP3, and MLKL.* J Biol Chem, 2013. **288**(43): p. 31268-79.
80. Murphy, J.M., P.E. Czabotar, J.M. Hildebrand, I.S. Lucet, J.G. Zhang, S. Alvarez-Diaz, R. Lewis, N. Lalaoui, D. Metcalf, A.I. Webb, S.N. Young, L.N. Varghese, G.M. Tannahill, E.C. Hatchell, I.J. Majewski, T. Okamoto, R.C. Dobson, D.J. Hilton, J.J. Babon, N.A. Nicola, A. Strasser, J. Silke, and W.S. Alexander, *The pseudokinase MLKL mediates necroptosis via a molecular switch mechanism.* Immunity, 2013. **39**(3): p. 443-53.
81. Vandenabeele, P., W. Declercq, F. Van Herreweghe, and T. Vanden Berghe, *The role of the kinases RIP1 and RIP3 in TNF-induced necrosis.* Sci Signal, 2010. **3**(115): p. re4.
82. Li, J., T. McQuade, A.B. Siemer, J. Napetschnig, K. Moriwaki, Y.S. Hsiao, E. Damko, D. Moquin, T. Walz, A. McDermott, F.K. Chan, and H. Wu, *The RIP1/RIP3 necrosome forms a functional amyloid signaling complex required for programmed necrosis.* Cell, 2012. **150**(2): p. 339-50.
83. Cho, Y.S., S. Challa, D. Moquin, R. Genga, T.D. Ray, M. Guildford, and F.K. Chan, *Phosphorylation-driven assembly of the RIP1-RIP3 complex regulates programmed necrosis and virus-induced inflammation.* Cell, 2009. **137**(6): p. 1112-23.
84. Maelfait, J., L. Liverpool, A. Bridgeman, K.B. Ragan, J.W. Upton, and J. Rehwinkel, *Sensing of viral and endogenous RNA by ZBP1/DAI induces necroptosis.* EMBO J, 2017. **36**(17): p. 2529-2543.

85. Cai, Z., S. Jitkaew, J. Zhao, H.C. Chiang, S. Choksi, J. Liu, Y. Ward, L.G. Wu, and Z.G. Liu, *Plasma membrane translocation of trimerized MLKL protein is required for TNF-induced necroptosis.* Nat Cell Biol, 2014. **16**(1): p. 55-65.
86. Gong, Y.N., C. Guy, H. Olauson, J.U. Becker, M. Yang, P. Fitzgerald, A. Linkermann, and D.R. Green, *ESCRT-III Acts Downstream of MLKL to Regulate Necroptotic Cell Death and Its Consequences.* Cell, 2017. **169**(2): p. 286-300 e16.
87. Yoon, S., A. Kovalenko, K. Bogdanov, and D. Wallach, *MLKL, the Protein that Mediates Necroptosis, Also Regulates Endosomal Trafficking and Extracellular Vesicle Generation.* Immunity, 2017. **47**(1): p. 51-65 e7.
88. Cai, Z., A. Zhang, S. Choksi, W. Li, T. Li, X.M. Zhang, and Z.G. Liu, *Activation of cell-surface proteases promotes necroptosis, inflammation and cell migration.* Cell Res, 2016. **26**(8): p. 886-900.
89. Xia, B., S. Fang, X. Chen, H. Hu, P. Chen, H. Wang, and Z. Gao, *MLKL forms cation channels.* Cell Res, 2016. **26**(5): p. 517-28.
90. Grootjans, S., T. Vanden Berghe, and P. Vandenabeele, *Initiation and execution mechanisms of necroptosis: an overview.* Cell Death Differ, 2017. **24**(7): p. 1184-1195.
91. Dondelinger, Y., P. Hulpiau, Y. Saeys, M.J.M. Bertrand, and P. Vandenabeele, *An evolutionary perspective on the necroptotic pathway.* Trends Cell Biol, 2016. **26**(10): p. 721-732.
92. Zhang, T., Y. Zhang, M. Cui, L. Jin, Y. Wang, F. Lv, Y. Liu, W. Zheng, H. Shang, J. Zhang, M. Zhang, H. Wu, J. Guo, X. Zhang, X. Hu, C.M. Cao, and R.P. Xiao, *CaMKII is a RIP3 substrate mediating ischemia- and oxidative stress-induced myocardial necroptosis.* Nat Med, 2016. **22**(2): p. 175-82.
93. Almyroudis, N.G., M.J. Grimm, B.A. Davidson, M. Rohm, C.F. Urban, and B.H. Segal, *NETosis and NADPH oxidase: at the intersection of host defense, inflammation, and injury.* Front Immunol, 2013. **4**: p. 45.
94. Hahn, S., S. Giaglis, C.S. Chowdhury, I. Hosli, and P. Hasler, *Modulation of neutrophil NETosis: interplay between infectious agents and underlying host physiology.* Semin Immunopathol, 2013. **35**(4): p. 439-53.
95. Yang, H., M.H. Biermann, J.M. Brauner, Y. Liu, Y. Zhao, and M. Herrmann, *New Insights into Neutrophil Extracellular Traps: Mechanisms of Formation and Role in Inflammation.* Front Immunol, 2016. **7**: p. 302.
96. Yipp, B.G. and P. Kubes, *NETosis: how vital is it?* Blood, 2013. **122**(16): p. 2784-94.
97. Schonrich, G. and M.J. Raftery, *Neutrophil Extracellular Traps Go Viral.* Front Immunol, 2016. **7**: p. 366.
98. Papayannopoulos, V., *Neutrophil extracellular traps in immunity and disease.* Nat Rev Immunol, 2018. **18**(2): p. 134-147.
99. Hakkim, A., B.G. Furnrohr, K. Amann, B. Laube, U.A. Abed, V. Brinkmann, M. Herrmann, R.E. Voll, and A. Zychlinsky, *Impairment of neutrophil extracellular trap degradation is associated with lupus nephritis.* Proc Natl Acad Sci U S A, 2010. **107**(21): p. 9813-8.
100. Kolaczkowska, E., C.N. Jenne, B.G. Surewaard, A. Thanabalasuriar, W.Y. Lee, M.J. Sanz, K. Mowen, G. Opdenakker, and P. Kubes, *Molecular mechanisms of NET formation and degradation revealed by intravital imaging in the liver vasculature.* Nat Commun, 2015. **6**: p. 6673.
101. Szretter, K.J., S. Gangappa, X. Lu, C. Smith, W.J. Shieh, S.R. Zaki, S. Sambhara, T.M. Tumpey, and J.M. Katz, *Role of host cytokine responses in the pathogenesis of avian H5N1 influenza viruses in mice.* J Virol, 2007. **81**(6): p. 2736-44.
102. Daidoji, T., T. Koma, A. Du, C.S. Yang, M. Ueda, K. Ikuta, and T. Nakaya, *H5N1 avian influenza virus induces apoptotic cell death in mammalian airway epithelial cells.* J Virol, 2008. **82**(22): p. 11294-307.

103. Uiprasertkul, M., R. Kitphati, P. Puthavathana, R. Kriwong, A. Kongchanagul, K. Ungchusak, S. Angkasekwinai, K. Chokephaibulkit, K. Srisook, N. Vanprapar, and P. Auewarakul, *Apoptosis and pathogenesis of avian influenza A (H5N1) virus in humans.* Emerg Infect Dis, 2007. **13**(5): p. 708-12.
104. Porto, B.N. and R.T. Stein, *Neutrophil Extracellular Traps in Pulmonary Diseases: Too Much of a Good Thing?* Front Immunol, 2016. **7**: p. 311.
105. Ichinohe, T., I.K. Pang, and A. Iwasaki, *Influenza virus activates inflammasomes via its intracellular M2 ion channel.* Nat Immunol, 2010. **11**(5): p. 404-10.
106. Ichinohe, T., H.K. Lee, Y. Ogura, R. Flavell, and A. Iwasaki, *Inflammasome recognition of influenza virus is essential for adaptive immune responses.* J Exp Med, 2009. **206**(1): p. 79-87.
107. Pang, I.K. and A. Iwasaki, *Inflammasomes as mediators of immunity against influenza virus.* Trends Immunol, 2011. **32**(1): p. 34-41.
108. Tate, M.D., J.D. Ong, J.K. Dowling, J.L. McAuley, A.B. Robertson, E. Latz, G.R. Drummond, M.A. Cooper, P.J. Hertzog, and A. Mansell, *Reassessing the role of the NLRP3 inflammasome during pathogenic influenza A virus infection via temporal inhibition.* Sci Rep, 2016. **6**: p. 27912.
109. Song, H., G.R. Nieto, and D.R. Perez, *A new generation of modified live-attenuated avian influenza viruses using a two-strategy combination as potential vaccine candidates.* J Virol, 2007. **81**(17): p. 9238-48.
110. CDC, *Estimating seasonal influenza-associated deaths in the United States*. 2017.
111. Salomon, R., E. Hoffmann, and R.G. Webster, *Inhibition of the cytokine response does not protect against lethal H5N1 influenza infection.* Proc Natl Acad Sci U S A, 2007. **104**(30): p. 12479-81.
112. Narasaraju, T., E. Yang, R.P. Samy, H.H. Ng, W.P. Poh, A.A. Liew, M.C. Phoon, N. van Rooijen, and V.T. Chow, *Excessive neutrophils and neutrophil extracellular traps contribute to acute lung injury of influenza pneumonitis.* Am J Pathol, 2011. **179**(1): p. 199-210.
113. Ferguson, N.M., D.A. Cummings, C. Fraser, J.C. Cajka, P.C. Cooley, and D.S. Burke, *Strategies for mitigating an influenza pandemic.* Nature, 2006. **442**(7101): p. 448-52.